On the Approximation of Electromagnetic Fields by Edge Finite Elements. Part 2: A Heterogeneous Multiscale Method for Maxwell's equations

Patrick Ciarlet, Sonia Fliss, Christian Stohrer

On the Approximation of Electromagnetic Fields by Edge Finite Elements. Part 2: A Heterogeneous Multiscale Method for Maxwell's equations

Patrick Ciarlet[a], Sonia Fliss[a], Christian Stohrer[b]

[a] *POEMS (CNRS/ENSTA ParisTech/INRIA), 828, Boulevard des Maréchaux, 91762 Palaiseau Cedex, France*
[b] *IANM 1 (Karlsruhe Institute of Technology), Englerstrasse 2, 76131 Karlsruhe, Germany*

Abstract

In the second part of this series of papers we consider highly oscillatory media. In this situation, the need for a triangulation that resolves all microscopic details of the medium makes standard edge finite elements impractical because of the resulting tremendous computational load. On the other hand, undersampling by using a coarse mesh might lead to inaccurate results. To overcome these difficulties and to improve the ratio between accuracy and computational costs, homogenization techniques can be used. In this paper we recall analytical homogenization results and propose a novel numerical homogenization scheme for Maxwell's equations in frequency domain. This scheme follows the design principles of heterogeneous multiscale methods. We prove convergence to the effective solution of the multiscale Maxwell's equations in a periodic setting and give numerical experiments in accordance to the stated results.

Keywords: Numerical Homogenization, Maxwell's equations, Heterogeneous Multiscale Method, Edge Finite Elements, Two-Scale Convergence, T-coercivity

1. Introduction

As in the first part [1] of the series entitled "On the Approximation of Electromagnetic Fields by Edge Finite Elements" we study the numerical approximation of electromagnetic fields governed by Maxwell's equations. Here, we are interested in materials that oscillate on a microscopic length scale η much smaller than the size of the computational domain. Such materials are modeled by their electric permittivity tensor ε^η and their magnetic permeability tensor μ^η. The microscopic nature of these materials properties are indicated by the superscript η.

Our goal is to approximate the macroscopic behavior of the electric field $\boldsymbol{e}^\eta$. To obtain a reliable approximation of it using standard edge finite elements, the microscopic details

Email addresses: patrick.ciarlet@ensta-paristech.fr (Patrick Ciarlet), sonia.fliss@ensta-paristech.fr (Sonia Fliss), christian.stohrer@kit.edu (Christian Stohrer)

in μ^η and ε^η need to be resolved. This leads to an enormous number of degrees of freedom and might result in infeasibly high computational costs. Therefore, more involved methods are needed. A standard approach consists in replacing the multiscale tensors μ^η and ε^η with effective ones not depending on the micro scale, such that the macroscopic properties of the unknown electric field remain unchanged. While mixing formulas, see [2] and the references therein, are often used in physics and engineering, homogenization results are more common in the mathematical literature. In the seminal book [3] homogenization results for elliptic equations involving a **curl-curl** operator where proven. This proof relies on a div-**curl** lemma and uses the technique of compensated compactness. Homogenization results of time-dependent Maxwell's equations can be found e.g. in [4] and in [5, 6]. In the later references the notion of two-scale convergence was used to justify rigorously the homogenization process. Using similar techniques in a frequency domain setting, homogenization for an electromagnetic scattering problem in the whole space by a multiscale obstacle was achieved in [7]. More recently, a novel corrector result for materials fulfilling a symmetry assumptions has been proven in [8]. In this article, we give a slightly different homogenization result based on two-scale convergence in the second part of Section 2. This is the basis upon which our numerical homogenization scheme is built.

The term "numerical homogenization" is used for numerical methods that approximate the effective or homogenized solution of a multiscale equation without knowing the exact effective parameters. The most fundamental numerical homogenization methods precompute numerically effective parameters not depending on the micro scale. In a second step, an approximated effective equation can be solved with standard methods. In [9] two such methods for Maxwell's equations are compared. The first one is based on the homogenization results as described above, while the second one is based on a Floquet-Bloch expansion, see [10]. While such methods are quite accessible, their range of application is usually limited to periodic settings without straightforward generalizations to more involved settings. In addition the influence of the numerical discretization error in the approximation of the effective parameters on the overall solution is hardly ever considered.

Novel numerical homogenization schemes, such as e.g. Multiscale Finite Element Methods (MsFEM) [11, 12] and Heterogeneous Multiscale Method (HMM) [13, 14] do not rely on a priori computation of the effective parameters to approximate the effective behavior. In this paper we follow the HMM framework to propose a novel numerical homogenization scheme for Maxwell's equations. A detailed description of our scheme can be found in Section 3. In [15, 16] an HMM scheme was applied to an Eddy current problem, but without rigorous convergence proof. There, the macro problem, which involves the **curl**-operator, was discretized with Lagrange finite elements and the introduction of a stabilization term was needed. By contrast, we use edge finite elements for the macro solver and prove an abstract a priori error bound in Section 4. Very recently another HMM scheme for Maxwell's equations was proposed in [17], where in similarity with our scheme, edge finite elements are used for the macro solver. Nevertheless, the two methods differ from each other. First of all, in [17] a problem with non-vanishing conductivity was considered, whereas in this article the conductivity equals zero. As a consequence, the Maxwell's equations are not coercive in our case. To overcome this additional difficulty we use the notion of T-coercivity [18, 19]. Secondly, their method relies on a divergence regularization and thus the micro problem for the permeability

differ from the micro problems we use. We will highlight the similarities and differences of these two HMM methods in more detail in the course of this article. In Section 5 we illustrate how to apply the general method and the error bounds to concrete settings. Numerical experiments corroborating the theoretical results are presented in Section 6.

1.1. Notation

Whenever possible we follow the notations of [1]. In the following we repeat the most important ones for the self-containment of this article and add some complementary ones. Let $\mathcal{O} \subset \mathbb{R}^3$ be an open, bounded connected set with Lipschitz boundary $\partial\mathcal{O}$ in $\mathbb{R}^3$, i.e. $\mathcal{O}$ is a domain. The standard orthonomal basis of $\mathbb{R}^3$ is denoted by $(\boldsymbol{e}_k)_{k=1,2,3}$ and the $d \times d$-identity matrix (with $d = 2$ or 3) by I_d.

We use the usual notation $H^\ell(\mathcal{O})$ for Sobolev spaces with the standard convention that $L^2(\mathcal{O}) = H^0(\mathcal{O})$. In addition we will denote their vector-valued counterparts in bold face, e.g. $\boldsymbol{H}^\ell(\mathcal{O}) := \big(H^\ell(\mathcal{O})\big)^3$. By $(\cdot \,|\, \cdot)_{\ell,\mathcal{O}}$, respectively $\|\cdot\|_{\ell,\mathcal{O}}$, we denote the standard scalar product, resp. the standard norm in $H^\ell(\mathcal{O})$ or $\boldsymbol{H}^\ell(\mathcal{O})$. Furthermore, we will use the notation $\boldsymbol{H}(\mathbf{curl};\mathcal{O})$ for $\boldsymbol{L}^2(\mathcal{O})$-measurable functions whose curl lays in the same function space. Its norm is given by

$$\|\boldsymbol{v}\|_{\mathbf{curl},\mathcal{O}} = \Big((\boldsymbol{v} \,|\, \boldsymbol{v})_{0,\mathcal{O}} + (\mathbf{curl}\,\boldsymbol{v} \,|\, \mathbf{curl}\,\boldsymbol{v})_{0,\mathcal{O}}\Big)^{1/2}.$$

The subspace of functions in $\boldsymbol{H}(\mathbf{curl};\mathcal{O})$ with vanishing tangential component on the boundary $\partial\mathcal{O}$ is denoted by $\boldsymbol{H}_0(\mathbf{curl};\mathcal{O})$. Note that $\boldsymbol{H}_0(\mathbf{curl};\mathcal{O})$ is the closure of $\boldsymbol{\mathcal{D}}(\mathcal{O})$ in $\boldsymbol{H}(\mathbf{curl};\mathcal{O})$. While for a cuboidal domain $\mathcal{O}$ periodic boundary conditions are widely used for Sobolev spaces, they are less common for $\boldsymbol{H}(\mathbf{curl};\mathcal{O})$. Similarly to $\boldsymbol{H}_0(\mathbf{curl};\mathcal{O})$, we let $\boldsymbol{H}_{\mathrm{per}}(\mathbf{curl};\mathcal{O})$ be the closure of $\boldsymbol{C}^\infty_{\mathrm{per}}(\mathcal{O})$ in $\boldsymbol{H}(\mathbf{curl};\mathcal{O})$, where $\boldsymbol{C}^\infty_{\mathrm{per}}(\mathcal{O})$ denotes the space of smooth $\mathcal{O}$-periodic functions restricted to $\mathcal{O}$. We proceed similarly to define $\boldsymbol{H}(\mathrm{div};\mathcal{O})$ for $\boldsymbol{L}^2(\mathcal{O})$-measurable functions whose divergence lays in the same function space, and the ad hoc subspaces $\boldsymbol{H}_0(\mathrm{div};\mathcal{O})$ and $\boldsymbol{H}_{\mathrm{per}}(\mathrm{div};\mathcal{O})$ (replace tangential component by normal component in the previous definition). In this article, periodic boundary conditions are mainly used for the centered unit cube $Y = (-1/2, 1/2)^3$ and its shifted and scaled version given by

$$Y_\delta(\boldsymbol{x}) := \boldsymbol{x} + (-\delta/2, \delta/2)^3$$

for $\delta > 0$ and $\boldsymbol{x} = (x_1, x_2, x_3)^T \in \mathbb{R}^3$.

For a vector space V with norm $\|\cdot\|_V$ and a map $T : V \to V$ the standard operator norm is denoted by $|||T|||$. We use the same notation for bilinear forms $B : V \times V \to \mathbb{R}$ as we set

$$|||B||| = \sup_{v,w \in V\setminus\{0\}} \frac{|B(v \,|\, w)|}{\|v\|_V \|w\|_V}.$$

For a function $\boldsymbol{v} : (\boldsymbol{x}, \boldsymbol{y}) \mapsto \boldsymbol{v}(\boldsymbol{x}, \boldsymbol{y})$, we write $\mathbf{curl}_{\boldsymbol{x}}\,\boldsymbol{v}$, resp. $\mathbf{curl}_{\boldsymbol{y}}\,\boldsymbol{v}$, for the curl of $\boldsymbol{v}$ taken with respect to the first, resp. the second variable. For other differential operators we use the same notation, e.g. $\mathrm{div}_{\boldsymbol{y}}\,\boldsymbol{v}$ denotes the divergence of $\boldsymbol{v}$ with respect to its second argument.

2. Model Problem and Analytical Homogenization

Let $\Omega \subset \mathbb{R}^3$ be a domain and denote by $\nu^\eta = (\mu^\eta)^{-1}$ the inverse of the magnetic permeability. The variational formulation of the second order, time-harmonic Maxwell's equations with solutions in $\boldsymbol{H}_0(\mathbf{curl};\Omega)$ is given by

$$\begin{cases} \textit{Find } \boldsymbol{e}^\eta \in \boldsymbol{H}_0(\mathbf{curl};\Omega) \textit{ such that} \\ (\nu^\eta \,\mathbf{curl}\, \boldsymbol{e}^\eta \,|\, \mathbf{curl}\, \boldsymbol{v})_{0,\Omega} - \omega^2(\varepsilon^\eta \boldsymbol{e}^\eta \,|\, \boldsymbol{v})_{0,\Omega} = (\boldsymbol{f} \,|\, \boldsymbol{v})_{0,\Omega} \qquad \forall \boldsymbol{v} \in \boldsymbol{H}_0(\mathbf{curl};\Omega), \end{cases} \tag{1}$$

with given pulsation $\omega > 0$ and source term $\boldsymbol{f} \in \boldsymbol{L}^2(\Omega)$. Because the bilinear form

$$\mathfrak{B}^\eta(\boldsymbol{v} \,|\, \boldsymbol{w}) = (\nu^\eta \,\mathbf{curl}\, \boldsymbol{v} \,|\, \mathbf{curl}\, \boldsymbol{w})_{0,\Omega} - \omega^2(\varepsilon^\eta \boldsymbol{v} \,|\, \boldsymbol{w})_{0,\Omega} \qquad \forall \boldsymbol{v}, \boldsymbol{w} \in \boldsymbol{H}_0(\mathbf{curl};\Omega) \tag{2}$$

is not coercive, the a priori error analysis in Section 4 is more involved than for standard FE-HMM schemes, see e.g. [14] and the references therein.

For simplicity of the presentation we restrict ourselves from now on to locally periodic functions, this means that there are ε and ν such that

$$\varepsilon^\eta(\boldsymbol{x}) = \varepsilon\Big(\boldsymbol{x}, \frac{\boldsymbol{x}}{\eta}\Big) \qquad \text{and} \qquad \nu^\eta(\boldsymbol{x}) = \nu\Big(\boldsymbol{x}, \frac{\boldsymbol{x}}{\eta}\Big) \tag{3}$$

for almost every $\boldsymbol{x} \in \Omega$, where ε and ν are both Y-periodic with respect to their second argument. Thus η is the oscillation length of the medium through which the electromagnetic wave is propagating. We would like to emphasize that the FE-HMM scheme presented in Section 3.3 can easily be generalized to more complicated situations. These generalizations are similar to the ones for FE-HMM schemes for other types of equations [20]. Let $\xi \in \{\varepsilon, \nu\}$, we make form now on the following regularity assumptions.

$$\text{The tensor } \xi \text{ is symmetric and in } \big(C(\Omega; L^\infty_{\mathrm{per}}(Y))\big)^{3\times 3}. \tag{A$_1$}$$

$$\begin{cases} \text{There are } \alpha, \beta > 0, \text{ such that for all } \boldsymbol{z} \in \mathbb{R}^3 \text{ and a.e. } (\boldsymbol{x}, \boldsymbol{y}) \in \Omega \times Y \\ \qquad\qquad \alpha|\boldsymbol{z}|^2 \le \xi(\boldsymbol{x}, \boldsymbol{y})\boldsymbol{z} \cdot \boldsymbol{z} \le \beta|\boldsymbol{z}|^2. \end{cases} \tag{A$_2$}$$

2.1. Well-posedness of the Model Problem

Suppose that assumptions (A$_1$) and (A$_2$) hold for ε and ν. It is well known that (1) is well-posed if, and only if, $\omega^2 \notin \Lambda^\eta$, where Λ^η is the set of eigenvalues of the eigenproblem associated to (1). More precisely, $\Lambda^\eta = \{\lambda_k^\eta\}_{k\in\mathbb{N}_0}$ with $0 \le \lambda_0^\eta \le \ldots \le \lambda_k^\eta \le \ldots$, where λ_k^η is a solution of the following eigenproblem.

$$\begin{cases} \textit{Find } (\boldsymbol{e}_k^\eta, \lambda_k^\eta) \in \big\{\boldsymbol{w} \in \boldsymbol{H}_0(\mathbf{curl};\Omega) : \mathrm{div}(\varepsilon^\eta \boldsymbol{w}) = 0\big\} \times \mathbb{R} \textit{ such that } \boldsymbol{e}_k^\eta \neq 0 \textit{ and} \\ \qquad (\nu^\eta \,\mathbf{curl}\, \boldsymbol{e}_k^\eta \,|\, \mathbf{curl}\, \boldsymbol{v})_{0,\Omega} = \lambda_k^\eta(\varepsilon^\eta \boldsymbol{e}_k^\eta \,|\, \boldsymbol{v})_{0,\Omega} \qquad \forall \boldsymbol{v} \in \boldsymbol{H}_0(\mathbf{curl};\Omega). \end{cases}$$

The well-posedness result can for example be shown using the notion of T-coercivity, see [19], where it has been shown that (1) is well-posed if and only if the corresponding continuous bilinear form $\mathfrak{B}^\eta$ defined in (2) is T-coercive.

Definition 1. Let $\boldsymbol{V}$ be a Hilbert space, a bilinear form $\mathfrak{B}$ defined over $\boldsymbol{V}$ is *T-coercive* if there exist $\alpha > 0$ and an isomorphism $T \in \mathcal{L}(\boldsymbol{V})$ such that

$$\big|\mathfrak{B}(\boldsymbol{v} \,|\, T\boldsymbol{v})\big| \ge \alpha \|\boldsymbol{v}\|^2_{\boldsymbol{V}}, \quad \forall \boldsymbol{v} \in \boldsymbol{V}.$$

In our case T-coercivity means, that there is a bijective map T^η from $\boldsymbol{H}_0(\mathbf{curl};\Omega)$ into itself and $c_{T^\eta} > 0$, such that

$$\mathfrak{B}^\eta(\boldsymbol{v} \,|\, T^\eta \boldsymbol{v}) \geq c_{T^\eta}\big((\nu^\eta \,\mathbf{curl}\, \boldsymbol{v} \,|\, \mathbf{curl}\, \boldsymbol{v})_{0,\Omega} + (\varepsilon^\eta \boldsymbol{v} \,|\, \boldsymbol{v})_{0,\Omega}\big). \tag{4}$$

In [19, Sec. 4.2] an explicit construction for a suitable map T^η is given under the assumptions (A_1) and (A_2). For this specific map it holds $|||T^\eta|||_{\mathbf{curl},\Omega} = 1$ and the coercivity constant c_{T^η} is given by

$$c_{T^\eta} = \inf_{\lambda^\eta \in \Lambda^\eta} \Big|\frac{\omega^2 - \lambda^\eta}{1 + \lambda^\eta}\Big|. \tag{5}$$

Note, that one could also use the Fredholm alternative instead of the T-coercivity to show that (1) is well-posed.

Remark 1. The right-hand side of (4) defines a norm equivalent to $\|\cdot\|_{\mathbf{curl},\Omega}$. In particular, there exists $C > 0$ such that

$$(\nu^\eta \,\mathbf{curl}\, \boldsymbol{v} \,|\, \mathbf{curl}\, \boldsymbol{v})_{0,\Omega} + (\varepsilon^\eta \boldsymbol{v} \,|\, \boldsymbol{v})_{0,\Omega} \geq C\|\boldsymbol{v}\|^2_{\mathbf{curl},\Omega}, \qquad \forall \boldsymbol{v} \in \boldsymbol{H}_0(\mathbf{curl};\Omega).$$

Because of the uniform ellipticity and boundedness of ε^η and ν^η the constant C does not depend on η.

2.2. Homogenization of Maxwell's equation

In this section we recall a homogenization result for the time-harmonic Maxwell's equations [7, 17], which we present in a slightly modified version fitting our purposes. This result can be summarized as follows: The electric field $\boldsymbol{e}^\eta$ of the multiscale problem converges weakly to $\boldsymbol{e}^{\mathrm{eff}}$, where $\boldsymbol{e}^{\mathrm{eff}}$ does not depend on the micro scale. Furthermore, $\boldsymbol{e}^{\mathrm{eff}}$ is the solution of an effective Maxwell's equations with electric permittivity $\varepsilon^{\mathrm{eff}}$ and inverse magnetic permeability ν^{eff}, that vary only on the macro scale. One of the proofs of the homogenization result relies on the notion of two-scale convergence [21, 22] for vector-valued functions, see [23, 7]. Let us recall its definition.

Definition 2. A sequence $\{\boldsymbol{e}^\eta\}$ in $\boldsymbol{L}^2(\Omega)$ *two-scale converges* to $\boldsymbol{e}^0 \in \boldsymbol{L}^2(\Omega \times Y)$ if

$$\lim_{\eta\to 0}\left(\boldsymbol{e}^\eta \,\middle|\, \boldsymbol{v}\Big(\cdot, \frac{\cdot}{\eta}\Big)\right)_{0,\Omega} = \int_\Omega \big(\boldsymbol{e}^0(\boldsymbol{x},\cdot) \,\big|\, \boldsymbol{v}(\boldsymbol{x},\cdot)\big)_{0,Y}\, d\boldsymbol{x}$$

for all $\boldsymbol{v} \in C_0^\infty\big(\Omega; \boldsymbol{C}^\infty_{\mathrm{per}}(Y)\big)$. We denote this convergence by $\boldsymbol{e}^\eta \overset{2\mathrm{s}}{\rightharpoonup} \boldsymbol{e}^0$.

Furthermore, we will use the following compactness result.

Proposition 1 (cf. [6, 7, 23]). *Let $(\boldsymbol{e}^\eta)_\eta$ be a uniformly bounded family in $\boldsymbol{H}(\boldsymbol{curl};\Omega)$. Then there is a two-scale convergent subsequence, still denoted by $(\boldsymbol{e}^\eta)_\eta$. This means that there is a function $\boldsymbol{e}^0(\boldsymbol{x},\boldsymbol{y}) \in \boldsymbol{L}^2(\Omega \times Y)$ such that*

$$\boldsymbol{e}^\eta(\boldsymbol{x}) \overset{2\mathrm{s}}{\rightharpoonup} \boldsymbol{e}^0(\boldsymbol{x},\boldsymbol{y}) \qquad \text{as } \eta \to 0.$$

This subsequence converges also weakly in $\boldsymbol{L}^2(\Omega)$ to the local mean of $\boldsymbol{e}^0$ over Y, i.e.

$$\boldsymbol{e}^\eta(\boldsymbol{x}) \rightharpoonup \boldsymbol{e}^{\mathrm{eff}}(\boldsymbol{x}) := \int_Y \boldsymbol{e}^0(\boldsymbol{x},\boldsymbol{y})\, d\boldsymbol{y} \qquad \text{weakly in } \boldsymbol{L}^2(\Omega).$$

Moreover,

$$\boldsymbol{curl}\, \boldsymbol{e}^{\eta}(\boldsymbol{x}) \rightharpoonup \boldsymbol{curl}\, \boldsymbol{e}^{\mathrm{eff}}(\boldsymbol{x}) \qquad \text{weakly in } \boldsymbol{L}^2(\Omega),$$

and there is $\boldsymbol{e}^1 \in L^2\big(\Omega; \boldsymbol{H}_{\mathrm{per}}(\boldsymbol{curl}, Y)\big)$ *such that*

$$\boldsymbol{curl}\, \boldsymbol{e}^{\eta}(\boldsymbol{x}) \overset{2\mathfrak{s}}{\rightharpoonup} \boldsymbol{curl}_{\boldsymbol{x}}\, \boldsymbol{e}^0(\boldsymbol{x}, \boldsymbol{y}) + \boldsymbol{curl}_{\boldsymbol{y}}\, \boldsymbol{e}^1(\boldsymbol{x}, \boldsymbol{y}).$$

From the same references we know that the limit $\boldsymbol{e}^0$ can be further decomposed as follows.

Corollary 2. *The difference between* $\boldsymbol{e}^0$ *and* $\boldsymbol{e}^{\mathrm{eff}}$ *is a conservative, periodic vector field. Hence, there is a scalar-valued-function* $\phi \in L^2\big(\Omega; H^1_{\mathrm{per}}(Y)\big)$ *such that*

$$\boldsymbol{e}^0(\boldsymbol{x}, \boldsymbol{y}) = \boldsymbol{e}^{\mathrm{eff}}(\boldsymbol{x}) + \nabla_{\boldsymbol{y}}\, \phi(\boldsymbol{x}, \boldsymbol{y})$$

for all $\boldsymbol{x} \in \Omega$.

Let us go back now to our multiscale problem. Following [3], we introduce two homogenization operators.

Definition 3. Let the tensor ξ be such that (A_1) and (A_2) hold. The *homogenization operator* $\mathcal{H}$ is given by

$$\big(\mathcal{H}(\xi)\big)(\boldsymbol{x}) := \int_Y \big(I_3 + D_{\boldsymbol{y}}^T \boldsymbol{\chi}^{\xi}(\boldsymbol{x}, \boldsymbol{y})\big)^T \xi(\boldsymbol{x}, \boldsymbol{y}) \big(I_3 + D_{\boldsymbol{y}}^T \boldsymbol{\chi}^{\xi}(\boldsymbol{x}, \boldsymbol{y})\big)\, d\boldsymbol{y},$$

where $D_{\boldsymbol{y}}^T$ denotes the transposed Jacobian with respect to $\boldsymbol{y}$, i.e.

$$\big(D_{\boldsymbol{y}}^T \boldsymbol{\chi}^{\xi}(\boldsymbol{x}, \boldsymbol{y})\big)_{i,j} = \partial_{\boldsymbol{y}_j} \chi_i^{\xi}, \qquad 1 \le i, j \le 3,$$

and $\boldsymbol{\chi}^{\xi} = (\chi_1^{\xi}, \chi_2^{\xi}, \chi_3^{\xi})^T$ is the vector-valued function whose entries are the solutions χ_k^{ξ} to the cell problem

$$\begin{cases} \text{Find } \chi_k^{\xi}(\boldsymbol{x}, \cdot) \in H^1_{\mathrm{per}}(Y), \text{ such that } \displaystyle\int_Y \chi_k^{\xi}(\boldsymbol{x}, \boldsymbol{y})\, d\boldsymbol{y} = 0 \text{ and} \\ \Big(\xi(\boldsymbol{x}, \cdot)\big(\boldsymbol{e}_k + \nabla_{\boldsymbol{y}}\, \chi_k^{\xi}(\boldsymbol{x}, \cdot)\big) \,\Big|\, \nabla\, \zeta\Big)_{0,Y} = 0, \text{ for all } \zeta \in H^1_{\mathrm{per}}(Y). \end{cases} \tag{6}$$

Note, that the homogenization operator $\mathcal{H}$ and the cell problem (6) are the same as for classical homogenization results, see e.g. [3, 4, 24]. It is well known, that $\mathcal{H}$ has the following properties.

Proposition 3. *If the tensor* ξ *satisfies the assumptions* (A_1) *and* (A_2)*, then* $\mathcal{H}(\xi)$ *is again symmetric, uniformly coercive and bounded with the same constants as* ξ *and we have the regularity* $\mathcal{H}(\xi) \in \big(C(\Omega)\big)^{3\times 3}$.

The second homogenization operator $\mathcal{K}$ defined below and the corresponding cell problem (7) are less commonly used.

Definition 4. Let the tensor ξ be such that (A_1) and (A_2) hold. The *homogenization operator* $\mathcal{K}$ is given by

$$\big(\mathcal{K}(\xi)\big)(\boldsymbol{x}) := \int_Y \big(I_3 + \mathbf{curl}_{\boldsymbol{y}}\, \boldsymbol{\theta}^\xi(\boldsymbol{x},\boldsymbol{y})\big)^T \xi(\boldsymbol{x},\boldsymbol{y}) \big(I_3 + \mathbf{curl}_{\boldsymbol{y}}\, \boldsymbol{\theta}^\xi(\boldsymbol{x},\boldsymbol{y})\big)\, d\boldsymbol{y},$$

where $\boldsymbol{\theta}^\xi = (\boldsymbol{\theta}_1^\xi, \boldsymbol{\theta}_2^\xi, \boldsymbol{\theta}_3^\xi)$ is the tensor whose columns are the solution $\boldsymbol{\theta}_k^\xi$ to the cell problem

$$\begin{cases} \textit{Find } (\boldsymbol{\theta}_k^\xi(\boldsymbol{x},\cdot), p) \in \boldsymbol{H}_{\mathrm{per}}(\mathbf{curl}; Y) \times H^1_{\mathrm{per}}(Y), \textit{ such that} \\ \displaystyle\int_Y \boldsymbol{\theta}_k^\xi(\boldsymbol{x},\boldsymbol{y})\, d\boldsymbol{y} = \mathbf{0}, \ \int_Y p(\boldsymbol{y})\, d\boldsymbol{y} = 0, \textit{ and} \\ \Big(\xi(\boldsymbol{x},\cdot)\big(\boldsymbol{e}_k + \mathbf{curl}_{\boldsymbol{y}}\, \boldsymbol{\theta}_k^\xi(\boldsymbol{x},\cdot)\big) \,\Big|\, \mathbf{curl}\, \boldsymbol{\zeta}\Big)_{0,Y} + \Big(\boldsymbol{\theta}_k^\xi(\boldsymbol{x},\cdot) \,\Big|\, \nabla\, q\Big)_{0,Y} + \Big(\boldsymbol{\zeta} \,\Big|\, \nabla\, p\Big)_{0,Y} = 0 \\ \textit{for all } (\boldsymbol{\zeta}, q) \in \boldsymbol{H}_{\mathrm{per}}(\mathbf{curl}; Y) \times H^1_{\mathrm{per}}(Y). \end{cases} \tag{7}$$

The curl of $\boldsymbol{\theta}^\xi$ is computed column-wise, i.e.

$$\big(\mathbf{curl}_{\boldsymbol{y}}\, \boldsymbol{\theta}^\xi(\boldsymbol{x},\boldsymbol{y})\big)_{i,j} = \big(\mathbf{curl}_{\boldsymbol{y}}\, \boldsymbol{\theta}_j^\xi(\boldsymbol{x},\boldsymbol{y})\big)_i, \qquad 1 \le i,j \le 3.$$

Some comments on the cell problem (7) are in order. Firstly, one checks easily that the Lagrange multiplier p vanishes by taking $\zeta = \nabla\, p$. Its introduction allows to handle the constraints on the divergence of $\boldsymbol{\theta}_k^\xi(\boldsymbol{x},\cdot)$ and on its normal trace (Gauge condition). We find $\boldsymbol{\theta}_k^\xi(\boldsymbol{x},\cdot) \in \boldsymbol{H}_{\mathrm{per}}(\mathrm{div}; Y)$ with $\mathrm{div}_{\boldsymbol{y}}\, \boldsymbol{\theta}_k^\xi(\boldsymbol{x},\cdot) = 0$. Secondly, the well-posedness of the cell problem (7) stems from the following lemma whose proof can be done by contradiction.

Lemma 4. *Define*

$$W(Y) = \big\{\boldsymbol{\zeta} \in \boldsymbol{H}_{\mathrm{per}}(\boldsymbol{curl}; Y) \,\big|\, (\boldsymbol{\zeta} \,|\, \nabla\, q)_{0,Y} = 0,\ \forall q \in H^1_{\mathrm{per}}(Y)\big\}.$$

Then there exists $C > 0$ such that

$$\|\boldsymbol{\zeta}\|_{0,Y} \le C \left\{ \|\boldsymbol{curl}\, \boldsymbol{\zeta}\|_{0,\Omega} + \left| \int_Y \boldsymbol{\zeta}\, d\boldsymbol{y} \right| \right\}, \qquad \forall \boldsymbol{\zeta} \in W(Y).$$

Lastly, we would like to note, that these two homogenization formulas are "dual" to each other in the following sense.

Lemma 5 (cf. [3, Chap. 1, Rem. 11.11]). *Let ξ be given such that (A_1) and (A_2) hold and the homogenization operators $\mathcal{H}$ and $\mathcal{K}$ be defined as above. Then*

$$\mathcal{K}(\xi) = \big(\mathcal{H}(\xi^{-1})\big)^{-1}.$$

Remark 2. Because of Lemma 5 the Proposition 3 holds true for $\mathcal{K}$, too.

Eventually, we can state the homogenized equation with the introduced notation.

$$\begin{cases} \textit{Find } \boldsymbol{e} \in \boldsymbol{H}_0(\mathbf{curl}; \Omega), \textit{ such that} \\ (\nu^{\mathrm{eff}}\, \mathbf{curl}\, \boldsymbol{e} \,|\, \mathbf{curl}\, \boldsymbol{v})_{0,\Omega} - \omega^2 (\varepsilon^{\mathrm{eff}} \boldsymbol{e} \,|\, \boldsymbol{v})_{0,\Omega} = (\boldsymbol{f} \,|\, \boldsymbol{v})_{0,\Omega}, \qquad \forall \boldsymbol{v} \in \boldsymbol{H}_0(\mathbf{curl}; \Omega), \end{cases} \tag{8}$$

with $\nu^{\text{eff}} = \mathcal{K}(\nu)$ and $\varepsilon^{\text{eff}} = \mathcal{H}(\varepsilon)$.

Let Λ^{eff} be the set of eigenvalues associated to the effective Maxwell's equations (8). Under the assumption

$$\omega^2 \notin \Lambda^{\text{eff}}, \tag{A$_3$}$$

the effective Maxwell's equations are well posed using again T-coercivty. Even more, (A$_3$) quarantees the well-posedness of (1) for all η small enough.

Lemma 6. *Suppose that ε and ν fulfill the assumptions* (A$_1$) *and* (A$_2$) *and that* (A$_3$) *holds. Then there is threshold value $\tilde{\eta} > 0$ such that* (1) *admits a unique solution $\boldsymbol{e}^\eta$ for all $\eta \leq \tilde{\eta}$. Moreover, these solutions $(\boldsymbol{e}^\eta)_\eta$ are uniformly bounded in $\boldsymbol{H}(\boldsymbol{curl}; \Omega)$.*

Proof. From Proposition 3 and Remark 2 it follows, that Λ^{eff} is discrete. Hence, we can write $\Lambda^{\text{eff}} = \left(\lambda_k^{\text{eff}}\right)_{k\in\mathbb{N}_0}$ with $\lambda_k^{\text{eff}} \leq \lambda_{k'}^{\text{eff}}$ for $k \leq k'$. Furthermore, assumption (A$_3$) is equivalent to

$$\gamma := \inf_{k\in\mathbb{N}_0} |\omega^2 - \lambda_k^{\text{eff}}| > 0.$$

From [25, Thm. 4.1] we know that Λ^η converges in a pointwise sense to Λ^{eff}. By contradiction, we find easily that

$$\exists \tilde{\eta} > 0, \quad \forall \eta \leq \tilde{\eta}, \qquad \inf_{\lambda^\eta \in \Lambda^\eta} |\omega^2 - \lambda^\eta| \geq \frac{\gamma}{2} \tag{9}$$

This means that $\omega^2 \notin \Lambda^\eta$ and it follows that (1) has a unique solution.

To prove that the solutions of (1) are uniformly bounded, we test it with $T^\eta \boldsymbol{e}^\eta$ and get

$$c_{T^\eta} C \|\boldsymbol{e}^\eta\|^2_{\mathbf{curl},\Omega} \leq \mathfrak{B}^\eta(\boldsymbol{e}^\eta \,|\, T^\eta \boldsymbol{e}^\eta) = (\boldsymbol{f} \,|\, T^\eta \boldsymbol{e}^\eta)_{0,\Omega} \leq \|\boldsymbol{f}\|_{0,\Omega} |||T^\eta|||_{\mathbf{curl},\Omega} \|\boldsymbol{e}^\eta\|_{0,\Omega}.$$

As mentioned before, $|||T^\eta|||_{\mathbf{curl},\Omega} = 1$ and C is independent of η according to (A$_2$). Thus it remains to bound c_{T^η} independently of η. If $\omega^2 > \lambda^\eta > 0$ if follows with (9) that

$$\frac{|\omega^2 - \lambda^\eta|}{1 + \lambda^\eta} \geq \frac{\gamma}{2 + 2\omega^2}$$

and if $0 < \omega^2 < \lambda^\eta$ we have because of (9) $\omega^2 + \frac{\gamma}{2} \leq \lambda^\eta$, wherefrom we get

$$\frac{|\omega^2 - \lambda^\eta|}{1 + \lambda^\eta} = 1 - \frac{1 + \omega^2}{1 + \lambda^\eta} \geq 1 - \frac{1 + \omega^2}{1 + \omega^2 + \frac{\gamma}{2}} = \frac{\gamma}{2 + 2\omega^2 + \gamma}.$$

Since γ is independent of η this finishes the proof with the help of (5). □

Because of this lemma, we can apply Proposition 1 to the set of solutions $(\boldsymbol{e}^\eta)_\eta$ of (1). Let $\boldsymbol{e}^0$, resp. $\boldsymbol{e}^{\text{eff}}$, be the corresponding two-scale, resp. weak $\boldsymbol{L}^2(\Omega)$ limit, of $(\boldsymbol{e}^\eta)_\eta$ as in Proposition 1. The following homogenization results for Maxwell's equations hold.

Theorem 7. *Let $(\boldsymbol{e}^\eta)_\eta$, $\boldsymbol{e}^0$, and $\boldsymbol{e}^{\text{eff}}$, be given as above. Under the assumption of Lemma 6, $\boldsymbol{e}^{\text{eff}}$ is the unique solution of* (8) *and the two-scale limit $\boldsymbol{e}^0$ is given by*

$$\boldsymbol{e}^0(\boldsymbol{x}, \boldsymbol{y}) = \left(I_3 + D_{\boldsymbol{y}}^T \boldsymbol{\chi}^\varepsilon(\boldsymbol{x}, \boldsymbol{y})\right) \boldsymbol{e}^{\text{eff}}(\boldsymbol{x})$$

where $\boldsymbol{\chi}^\varepsilon = (\chi_1^\varepsilon, \chi_2^\varepsilon, \chi_3^\varepsilon)^T$ is defined by (6).

For completeness, we present the proof, which shares a lot of similarities with the ones in [7] and [17].

PROOF. As already mentioned, we can apply Proposition 1 due to the uniform boundedness of $(\boldsymbol{e}^\eta)_\eta$. In addition to $\boldsymbol{e}^{\text{eff}}$ and $\boldsymbol{e}^0$, let also $\boldsymbol{e}^1$ be given as in Proposition 1. First, we test (1) with $\boldsymbol{v}(\boldsymbol{x}) = \eta \boldsymbol{w}(\boldsymbol{x})\zeta(\boldsymbol{x}/\eta)$ with $\boldsymbol{w} \in \boldsymbol{C}_0^\infty(\Omega)$ and $\zeta \in H^1_{\text{per}}(Y)$. Passing to the two-scale limit it follows that

$$\int_Y \nu(\boldsymbol{x},\boldsymbol{y})\big(\mathbf{curl}_{\boldsymbol{x}}\, \boldsymbol{e}^0(\boldsymbol{x},\boldsymbol{y}) + \mathbf{curl}_{\boldsymbol{y}}\, \boldsymbol{e}^1(\boldsymbol{x},\boldsymbol{y})\big) \times \nabla_{\boldsymbol{y}}\, \zeta(\boldsymbol{y})\, d\boldsymbol{y} = \boldsymbol{0}. \tag{10}$$

For readability, we introduce the abbreviation

$$\boldsymbol{r}(\boldsymbol{x},\boldsymbol{y}) := \nu(\boldsymbol{x},\boldsymbol{y})\big(\mathbf{curl}_{\boldsymbol{x}}\, \boldsymbol{e}^0(\boldsymbol{x},\boldsymbol{y}) + \mathbf{curl}_{\boldsymbol{y}}\, \boldsymbol{e}^1(\boldsymbol{x},\boldsymbol{y})\big).$$

Next, we use $\boldsymbol{v}(\boldsymbol{x}) = \rho(\boldsymbol{x})(\nabla\,\zeta)(\boldsymbol{x}/\eta)$ as test function with $\rho \in C_0^\infty(\Omega)$ and we consider the different terms in (1) separately. For the right-hand side, one can show that $(\boldsymbol{f} \,|\, \boldsymbol{v})_{0,\Omega} \to 0$ as $\eta \to 0$. For the first term on the left-hand side we have as $\eta \to 0$,

$$(\nu^\eta\, \mathbf{curl}\, \boldsymbol{e}^\eta \,|\, \mathbf{curl}\, \boldsymbol{v})_{0,\Omega} \to -\int_\Omega \nabla\, \rho(\boldsymbol{x}) \cdot \int_Y \boldsymbol{r}(\boldsymbol{x},\boldsymbol{y}) \times \nabla_{\boldsymbol{y}}\, \zeta(\boldsymbol{y})\, d\boldsymbol{y}\, d\boldsymbol{x} = 0$$

due to (10). Thus, $\lim_{\eta\to 0}(\varepsilon^\eta \boldsymbol{e}^\eta \,|\, \boldsymbol{v})_{0,\Omega} = 0$, from where

$$\int_Y \varepsilon(\boldsymbol{x},\boldsymbol{y})\boldsymbol{e}^0(\boldsymbol{x},\boldsymbol{y}) \cdot \nabla_{\boldsymbol{y}}\, \zeta(\boldsymbol{y})\, d\boldsymbol{y} = 0$$

follows. From Corollary 2, we know that there is $\phi \in L^2\big(\Omega; H^1_{\text{per}}(Y)\big)$ such that $\boldsymbol{e}^0(\boldsymbol{x},\boldsymbol{y}) = \boldsymbol{e}^{\text{eff}}(\boldsymbol{x}) + \nabla_{\boldsymbol{y}}\, \phi(\boldsymbol{x},\boldsymbol{y})$. We insert this into the last equation, to get because of the definition of $\boldsymbol{\chi}^\varepsilon$

$$\nabla_{\boldsymbol{y}}\, \phi(\boldsymbol{x},\boldsymbol{y}) = D_{\boldsymbol{y}}^T \boldsymbol{\chi}^\varepsilon(\boldsymbol{x},\boldsymbol{y}) \boldsymbol{e}^{\text{eff}}(\boldsymbol{x}),$$

which proves the characterization of $\boldsymbol{e}^0$. It remains to show, that $\boldsymbol{e}^{\text{eff}}$ solves (8).

To do so, we test (1) with a test functions $\boldsymbol{v}$ that does not depend on the micro scale. In the limit we get

$$\Big(\int_Y \boldsymbol{r}(\cdot,\boldsymbol{y})\, d\boldsymbol{y} \,\Big|\, \mathbf{curl}\, \boldsymbol{v}\Big)_{0,\Omega} - \omega^2 \Big(\int_Y \varepsilon(\cdot,\boldsymbol{y})\boldsymbol{e}^0(\cdot,\boldsymbol{y})\, d\boldsymbol{y} \,\Big|\, \boldsymbol{v}\Big)_{0,\Omega} = (\boldsymbol{f} \,|\, \boldsymbol{v})_{0,\Omega}.$$

Inserting the characterization of $\boldsymbol{e}^0$ into the second integral we find

$$\int_Y \varepsilon(\boldsymbol{x},\boldsymbol{y})\boldsymbol{e}^0(\boldsymbol{x},\boldsymbol{y})\, d\boldsymbol{y} = \int_Y \varepsilon(\boldsymbol{x},\boldsymbol{y})\big(I_3 + D_{\boldsymbol{y}}^T \boldsymbol{\chi}^\varepsilon(\boldsymbol{x},\boldsymbol{y})\big)\, d\boldsymbol{y} = \mathcal{H}(\varepsilon)\boldsymbol{e}^{\text{eff}}(\boldsymbol{x}),$$

where we used the definition of $\mathcal{H}$ and that

$$\int_Y \big(D_{\boldsymbol{y}}^T \boldsymbol{\chi}^\varepsilon(\boldsymbol{x},\boldsymbol{y})\big)^T \varepsilon(\boldsymbol{x},\boldsymbol{y})\big(I_3 + D_{\boldsymbol{y}}^T \boldsymbol{\chi}^\varepsilon(\boldsymbol{x},\boldsymbol{y})\big)\, d\boldsymbol{y} = 0,$$

due to the definition (6) of $\boldsymbol{\chi}^\varepsilon$. The computation of the first integral is a little trickier. Note first, that because of (10) there is a scalar-valued function $\rho(\boldsymbol{x},\boldsymbol{y})$, Y-periodic in its second argument, such that we can write $\boldsymbol{r}$ as

$$\boldsymbol{r}(\boldsymbol{x},\boldsymbol{y}) = \int_Y \boldsymbol{r}(\boldsymbol{x},\boldsymbol{y})\, d\boldsymbol{y} + \nabla_y\, \rho(\boldsymbol{x},\boldsymbol{y})$$

and by definition of $\boldsymbol{r}$, we have

$$(\nu^{-1}(\boldsymbol{x},\boldsymbol{y})\boldsymbol{r}(\boldsymbol{x},\boldsymbol{y}) \,|\, \nabla\,\zeta)_{0,Y} = 0 \qquad \forall \zeta \in H^1_{\mathrm{per}}(Y).$$

Taken together it follows that

$$\boldsymbol{r}(\boldsymbol{x},\boldsymbol{y}) = \big(I_3 + D^T_{\boldsymbol{y}}\boldsymbol{\chi}^{\nu^{-1}}(\boldsymbol{x},\boldsymbol{y})\big) \int_Y \boldsymbol{r}(\boldsymbol{x},\hat{\boldsymbol{y}})\, d\hat{\boldsymbol{y}}.$$

Therewith, we compute

$$\begin{aligned}
\mathcal{H}(\nu^{-1}) \int_Y \boldsymbol{r}(\boldsymbol{x},\boldsymbol{y})\, d\boldsymbol{y} &= \int_Y \nu^{-1}(\boldsymbol{x},\boldsymbol{y})\boldsymbol{r}(\boldsymbol{x},\boldsymbol{y})\, d\boldsymbol{y} \\
&= \int_Y \mathbf{curl}_{\boldsymbol{x}}\, \boldsymbol{e}^0(\boldsymbol{x},\boldsymbol{y}) + \mathbf{curl}_{\boldsymbol{y}}\, \boldsymbol{e}^1(\boldsymbol{x},\boldsymbol{y})\, d\boldsymbol{y} \\
&= \mathbf{curl}\, \boldsymbol{e}^{\mathrm{eff}}(\boldsymbol{x}),
\end{aligned}$$

where we used the definition of $\mathcal{H}$ in the first and the one of $\boldsymbol{r}$ in the second equality. For the third equality we used the characterization of $\boldsymbol{e}^0$ and the fact that the integral of the divergence and the curl of a periodic function over one period vanishes. An application of the dual formula, see Lemma 5, finishes the proof. □

Remark 3. In contrast to homogenization of second order elliptic PDEs, we do not have strong convergence in general. Qualitatively the behavior of $\boldsymbol{e}^\eta$ for a sequence of diminishing values of η can be described as follows. While the length of the oscillations in $\boldsymbol{e}^\eta$ tends to zero, the amplitude does not decay but stays bounded. This coincides with the fact that the two scale limit $\boldsymbol{e}^0$ depends not only on $\boldsymbol{x}$ but also on $\boldsymbol{y}$.

We conclude this section by comparing Theorem 7 to the results in [7] and [17]. In the first of these references a scattering problem is considered. We see, that the effective permittivity $\varepsilon^{\mathrm{eff}}$ is given exactly in the same way. On the other hand, they give a formulation for the effective permeability μ^{eff} and not ν^{eff}. In this instance, this is the natural choice since the first order formulation of Maxwell's equations are considered. It is shown, that $\mu^{\mathrm{eff}} = \mathcal{H}(\mu)$ which is in total agreement which our result, since one has

$$(\mu^{\mathrm{eff}})^{-1} = \big(\mathcal{H}(\mu)\big)^{-1} = \mathcal{K}(\mu^{-1}) = \mathcal{K}(\nu) = \nu^{\mathrm{eff}}$$

due to Lemma 5. We prefer the formulation with $\mathcal{K}$ as we consider the second order formulation of Maxwell's equations. This homogenization operator allows us to construct a multiscale scheme without the need of inverting the effective magnetic permeability.

If one sets the conductivity to zero in the formula for the homogenized matrices given in [17], one retrieves again the same formula for the effective permittivity. Moreover, up to the divergence-regularization term the formula for the effective permeability and the corresponding cell problem coincide with the results stated above. This regularization term was introduced artificially to get rid of the divergence-free condition in the cell problem (7) for the permeability. In this respect, our approach differs essentially. We keep the more intuitive homogenization result without additional regularization, but we have still to take care of the divergence-free condition in the definition of our algorithm, see (7).

3. Multiscale Scheme

Our FE-HMM for Maxwell's equations follows the general methodology described in [14, Sec. 4]. We start by giving a short overlook of the whole algorithm. Like every HMM scheme, our method can be decoupled into two different levels. The solver on the macroscopic level approximates the solution of the effective Maxwell's equations (8). We use standard $\boldsymbol{H}(\mathbf{curl};\Omega)$-conforming edge elements for the discretization, i.e. Nédélec's first family edge elements. In addition we choose a quadrature formula for the calculation of integrals on the macroscopic level. Since the effective permittivity $\varepsilon^{\text{eff}} = \mathcal{H}(\varepsilon)$ and the effective inverse permeability $\nu^{\text{eff}} = \mathcal{K}(\nu)$ are not known a priori, we need two micro solvers to estimate the missing data. More precisely, two micro problems connected to the macroscopic solution through coupling constraints are solved numerically around every macroscopic quadrature point. In the rest of this section we give a detailed description of our multiscale scheme. We first address all the ingredients of the method in Sections 3.1 and 3.2, before combining them to form the complete algorithm, given in Section 3.3.

3.1. Macroscale solver

For the ease of exposition, let Ω be a a Lipschitz polyhedron such that it can be triangulated by a shape regular family of tetrahedral meshes $(\mathcal{T}_H)_H$. Let H_K be the diameter of a simplicial element $K \in \mathcal{T}_H$ and set $H = \max_{K\in\mathcal{T}_H} H_K$. These (macroscopic) meshes do not need to resolve the micro scale structure of the medium. On the contrary $H \gg \eta$ is allowed and desired. Furthermore, let $\boldsymbol{V}_{H,0}$ be a finite dimensional edge element subspace of $\boldsymbol{H}_0(\mathbf{curl};\Omega)$ belonging to Nédélec's first family, of given order.

For every $K \in \mathcal{T}_H$ we choose a quadrature formula $(\boldsymbol{x}_{K,j}, \omega_{K,j})_{j=1}^{J_K}$ to evaluate integrals on K given by its nodes $\boldsymbol{x}_{K,j}$ and weights $\omega_{K,j}$. If ε^{eff} and ν^{eff} were known, we could approximate the solution to the effective Maxwell's equations (8) by

$$\begin{cases} \textit{Find } \boldsymbol{e}_H^{\text{eff}} \in \boldsymbol{V}_{H,0}\textit{, such that} \\ \big(\nu^{\text{eff}}\,\mathbf{curl}\,\boldsymbol{v}_H \,\big|\, \mathbf{curl}\,\boldsymbol{w}_H\big)_H - \omega^2\big(\varepsilon^{\text{eff}}\boldsymbol{v}_H \,\big|\, \boldsymbol{w}_H\big)_H = (\boldsymbol{f}\,|\,\boldsymbol{v}_H)_{0,\Omega}, \qquad \forall \boldsymbol{v}_H \in \boldsymbol{V}_{H,0}, \end{cases} \tag{11}$$

where the $\boldsymbol{L}^2(\Omega)$ scalar product is evaluated by

$$(\boldsymbol{v}_H \,|\, \boldsymbol{w}_H)_H := \sum_{K\in\mathcal{T}_H} \sum_{j=1}^{J_K} \omega_{K,j} \boldsymbol{v}_H(\boldsymbol{x}_{K,j}) \cdot \boldsymbol{w}_H(\boldsymbol{x}_{K,j}).$$

Note, that (11) is nothing else than a standard FE discretization of (8) with numerical integration. In order to have a meaningful scheme, $(\cdot\,|\,\cdot)_H$ should be a sufficiently accurate approximation of the $\boldsymbol{L}^2(\Omega)$ scalar product. The precise assumption is explained later—it is assumption (Q) in Theorem 11.

Remark 4. To integrate the source term $\boldsymbol{f}$ we use the exact scalar product and not its approximation. This is only to simplify the presentation of our results. Without any conceptual changes, we could use an approximated scalar product for the source term as well. This would lead only to an additive error term in Theorem 10 and 11.

To improve the readability, we introduce the bilinear form $B_H^{\text{eff}}(\cdot\,|\,\cdot)$ given by

$$B_H^{\text{eff}}(\boldsymbol{v}_H \,|\, \boldsymbol{w}_H) = \big(\nu^{\text{eff}}\,\mathbf{curl}\,\boldsymbol{v}_H \,\big|\, \mathbf{curl}\,\boldsymbol{w}_H\big)_H, \qquad \forall \boldsymbol{v}_H, \boldsymbol{w}_H \in \boldsymbol{V}_{H,0}.$$

We would like to stress that this bilinear form is never actually used in the implementation of our FE-HMM scheme. However, in the a priori error analysis it will be of great use. Especially the reformulation in the lemma stated below helps getting an inside view of the FE-HMM scheme.

Lemma 8. *Let the assumptions* (A$_1$)–(A$_3$) *hold. For* $\boldsymbol{v}_H \in \boldsymbol{V}_{H,0}$*, let the function* $\boldsymbol{v}$ *solve*

$$\begin{cases} \text{Find } \big(\boldsymbol{v}(\boldsymbol{x}_{K,j},\cdot),p\big) \in \big(\boldsymbol{v}_{H,\mathrm{lin}} + \boldsymbol{H}_{\mathrm{per}}(\boldsymbol{curl};Y_\eta(\boldsymbol{x}_{K,j}))\big) \times H^1_{\mathrm{per}}(Y_\eta(\boldsymbol{x}_{K,j})), \\ \text{such that } \displaystyle\int_{Y_\eta(\boldsymbol{x}_{K,j})} \boldsymbol{v}(\boldsymbol{x}_{K,j},\boldsymbol{x})\,d\boldsymbol{x} = \boldsymbol{0},\ \int_{Y_\eta(\boldsymbol{x}_{K,j})} p(\boldsymbol{x})\,d\boldsymbol{x} = 0, \text{ and} \\ \Big(\nu\Big(\boldsymbol{x}_{K,j},\frac{\cdot}{\eta}\Big)\,\boldsymbol{curl}_{\boldsymbol{y}}\,\boldsymbol{v}(\boldsymbol{x}_{K,j},\cdot)\,\Big|\,\boldsymbol{curl}\,\boldsymbol{\zeta}\Big)_{0,Y_\eta(\boldsymbol{x}_{K,j})} + \\ \qquad\qquad \Big(\boldsymbol{v}(\boldsymbol{x}_{K,j},\cdot)\,\Big|\,\nabla q\Big)_{0,Y_\eta(\boldsymbol{x}_{K,j})} + \Big(\boldsymbol{\zeta}\,\Big|\,\nabla p\Big)_{0,Y_\eta(\boldsymbol{x}_{K,j})} = 0, \\ \text{for all } (\boldsymbol{\zeta},q) \in \boldsymbol{H}_{\mathrm{per}}(\boldsymbol{curl};Y_\eta(\boldsymbol{x}_{K,j})) \times H^1_{\mathrm{per}}(Y_\eta(\boldsymbol{x}_{K,j})), \end{cases} \tag{12}$$

with

$$\boldsymbol{v}_{H,\mathrm{lin}}(\boldsymbol{x}) := \boldsymbol{v}_H(\boldsymbol{x}_{K,j}) + \frac{1}{2}\,\boldsymbol{curl}\,\boldsymbol{v}_H(\boldsymbol{x}_{K,j}) \times (\boldsymbol{x}-\boldsymbol{x}_{K,j}). \tag{13}$$

Similarly for $\boldsymbol{w}_H \in \boldsymbol{V}_{H,0}$*, let the function* $\boldsymbol{w}$ *be given in the same way replacing* $\boldsymbol{v}_H$ *with* $\boldsymbol{w}_H$ *in* (12)–(13)*. Then it holds*

$$B_H^{\mathrm{eff}}(\boldsymbol{v}_H \,|\, \boldsymbol{w}_H) = \sum_{K\in\mathcal{T}_H}\sum_{j=1}^{J_K} \frac{\omega_{K,j}}{|Y_\eta|}\Big(\nu\Big(\boldsymbol{x}_{K,j},\frac{\cdot}{\eta}\Big)\,\boldsymbol{curl}_{\boldsymbol{y}}\,\boldsymbol{v}(\boldsymbol{x}_{K,j},\cdot)\,\Big|\,\boldsymbol{curl}_{\boldsymbol{y}}\,\boldsymbol{w}(\boldsymbol{x}_{K,j},\cdot)\Big)_{0,Y_\eta(\boldsymbol{x}_{K,j})}. \tag{14}$$

Before proving this lemma, we highlight some important properties of $\boldsymbol{v}_{H,\mathrm{lin}}$. The curl and the divergence of $\boldsymbol{v}_{H,\mathrm{lin}}$ are constant. Even more, we have

$$\mathbf{curl}\,\boldsymbol{v}_{H,\mathrm{lin}}(\boldsymbol{x}) = \mathbf{curl}\,\boldsymbol{v}_H(\boldsymbol{x}_{K,j}) \tag{15}$$

and

$$\operatorname{div}\boldsymbol{v}_{H,\mathrm{lin}}(\boldsymbol{x}) = 0$$

for all $\boldsymbol{x} \in Y_\eta(\boldsymbol{x}_{K,j})$. Let q be in $H^1_{\mathrm{per}}(Y_\eta)$. Since $\boldsymbol{v}_{H,\mathrm{lin}}$ is divergence-free, an easy computation reveals

$$\big(\boldsymbol{v}_{H,\mathrm{lin}}\,\big|\,\nabla q\big)_{Y_\eta(\boldsymbol{x}_{K,j})} = \int_{\partial Y_\eta(\boldsymbol{x}_{K,j})} \boldsymbol{v}_{H,\mathrm{lin}}(\boldsymbol{x}) q(\boldsymbol{x}) \cdot \boldsymbol{n}(\boldsymbol{x})\,dS(\boldsymbol{x}) = 0, \tag{16}$$

where $\boldsymbol{n}(\boldsymbol{x})$ is the outer normal unit vector for $Y_\eta(\boldsymbol{x}_{K,j})$ at $\boldsymbol{x}$.

Proof (Lemma 8). To shorten the notation in this proof, we write only Y_η instead

$Y_\eta(\boldsymbol{x}_{K,j})$. Let $\boldsymbol{z}$ be a constant vector in $\mathbb{R}^3$ and consider the problem

$$\begin{cases} \textit{Find } (\tilde{\boldsymbol{v}}(\boldsymbol{x}_{K,j},\cdot),p) \in \boldsymbol{H}_{\mathrm{per}}(\mathbf{curl};Y_\eta)\times H^1_{\mathrm{per}}(Y_\eta), \\ \textit{such that } \displaystyle\int_{Y_\eta} \tilde{\boldsymbol{v}}(\boldsymbol{x}_{K,j},\boldsymbol{x})\,d\boldsymbol{x} = \mathbf{0},\ \int_{Y_\eta} p(\boldsymbol{x})\,d\boldsymbol{x} = 0,\ \textit{and} \\ \Big(\nu\Big(\boldsymbol{x}_{K,j},\frac{\cdot}{\eta}\Big)\big(\boldsymbol{z}+\mathbf{curl}_{\boldsymbol{y}}\,\tilde{\boldsymbol{v}}(\boldsymbol{x}_{K,j},\cdot)\big)\,\Big|\,\mathbf{curl}\,\boldsymbol{\zeta}\Big)_{0,Y_\eta} + \\ \qquad\qquad \Big(\tilde{\boldsymbol{v}}(\boldsymbol{x}_{K,j},\cdot)\,\Big|\,\nabla\, q\Big)_{0,Y_\eta} + \Big(\boldsymbol{\zeta}\,\Big|\,\nabla\, p\Big)_{0,Y_\eta} = 0, \\ \textit{for all } (\boldsymbol{\zeta},q)\in \boldsymbol{H}_{\mathrm{per}}(\mathbf{curl};Y_\eta)\times H^1_{\mathrm{per}}(Y_\eta). \end{cases} \tag{17}$$

which admits a unique solution according to Lemma 4. If $\boldsymbol{z}$ is the k-th basis vector $\boldsymbol{e}_k$ for $1\le k\le 3$, the solution can be written as

$$\tilde{\boldsymbol{v}}(\boldsymbol{x}_{K,j},\boldsymbol{x}) = \eta\boldsymbol{\theta}^\nu_k\Big(\boldsymbol{x}_{K,j},\frac{\boldsymbol{x}-\boldsymbol{x}_{K,j}}{\eta}\Big),$$

where $\boldsymbol{\theta}^\nu_k$ is the solution of the cell problem (7). Due to the linearity of (17), we have for a general $\boldsymbol{z}=(z_1,z_2,z_3)^T\in\mathbb{R}^3$ the representation

$$\tilde{\boldsymbol{v}}(\boldsymbol{x}_{K,j},\boldsymbol{x}) = \eta\sum_{k=1}^3 \boldsymbol{\theta}^\nu_k\Big(\boldsymbol{x}_{K,j},\frac{\boldsymbol{x}-\boldsymbol{x}_{K,j}}{\eta}\Big)z_k.$$

Because of the properties (15) and (16)

$$\boldsymbol{v}(\boldsymbol{x}_{K,j},\cdot) - \boldsymbol{v}_{H,\mathrm{lin}} + \frac{1}{|Y_\eta|}\int_{Y_\eta}\boldsymbol{v}_{H,\mathrm{lin}}(\boldsymbol{y})\,d\boldsymbol{y}$$

with $\boldsymbol{v}$ and $\boldsymbol{v}_{H,\mathrm{lin}}$ defined by (12) and (13), respectively, solves (17) with

$$\boldsymbol{z} = \mathbf{curl}\,\boldsymbol{v}_H(\boldsymbol{x}_{K,j}).$$

Then, $\boldsymbol{v}$ can be written as

$$\begin{aligned}\boldsymbol{v}(\boldsymbol{x}_{K,j},\boldsymbol{x}) = \boldsymbol{v}_{H,\mathrm{lin}}(\boldsymbol{x}) - \frac{1}{|Y_\eta|}\int_{Y_\eta}\boldsymbol{v}_{H,\mathrm{lin}}(\boldsymbol{y})\,d\boldsymbol{y} + \\ \eta\sum_{k=1}^3\boldsymbol{\theta}^\nu_k\Big(\boldsymbol{x}_{K,j},\frac{\boldsymbol{x}-\boldsymbol{x}_{K,j}}{\eta}\Big)\big(\mathbf{curl}\,\boldsymbol{v}_H(\boldsymbol{x}_{K,j})\big)_k.\end{aligned} \tag{18}$$

Additionally, we find

$$\mathbf{curl}_{\boldsymbol{y}}\,\boldsymbol{v}(\boldsymbol{x}_{K,j},\boldsymbol{x}) = \Big(I_3 + \mathbf{curl}_{\boldsymbol{y}}\,\boldsymbol{\theta}^\nu\Big(\boldsymbol{x}_{K,j},\frac{\boldsymbol{x}-\boldsymbol{x}_{K,j}}{\eta}\Big)\Big)\,\mathbf{curl}\,\boldsymbol{v}_H(\boldsymbol{x}_{K,j}).$$

The same formulas hold for $\boldsymbol{w}$ as well. Using the substitution $\boldsymbol{y} = {}^{(\boldsymbol{x}-\boldsymbol{x}_{K,j})}/_{\eta}$ together with the periodicity assumption of ν in its second argument, it is now easy to see that

$$\begin{gathered}\Big(\nu\Big(\boldsymbol{x}_{K,j},\frac{\cdot}{\eta}\Big)\,\mathbf{curl}_{\boldsymbol{y}}\,\boldsymbol{v}(\boldsymbol{x}_{K,j},\cdot)\,\Big|\,\mathbf{curl}_{\boldsymbol{y}}\,\boldsymbol{w}(\boldsymbol{x}_{K,j},\cdot)\Big)_{0,Y_\eta(\boldsymbol{x}_{K,j})} \\ = \\ \mathbf{curl}\,\boldsymbol{w}_H(\boldsymbol{x}_{K,j})^T\Big(|Y_\eta|\nu^{\mathrm{eff}}(\boldsymbol{x}_{K,j})\Big)\,\mathbf{curl}\,\boldsymbol{v}_H(\boldsymbol{x}_{K,j}),\end{gathered}$$

where $\nu^{\text{eff}} = \mathcal{K}(\nu)$ with the homogenization operator $\mathcal{K}$ from Definition 4. Inserting this into (14) finishes the proof. □

Remark 5. We have some freedom in the choice of $\boldsymbol{v}_{H,\text{lin}}$. The only properties needed in the proof are (15) and (16). Every other function having these properties could be used as well.

A similar reformulation holds for the effective permittivity.

Lemma 9. *Let the assumptions* (A_1)–(A_3) *hold. For* $\boldsymbol{v}_H \in \boldsymbol{V}_{H,0}$*, let the function* φ *solve*

$$\begin{cases} \text{Find } \varphi(\boldsymbol{x}_{K,j},\cdot) \in \varphi_{H,\text{lin}} + H^1_{\text{per}}\big(Y_\eta(\boldsymbol{x}_{K,j})\big), \text{ such that } \displaystyle\int_{Y_\eta(\boldsymbol{x}_{K,j})} \varphi(\boldsymbol{x}_{K,j},\boldsymbol{x})\,d\boldsymbol{x} = 0 \text{ and} \\ \qquad \Big(\varepsilon\Big(\boldsymbol{x}_{K,j},\frac{\cdot}{\eta}\Big)\nabla_{\boldsymbol{y}}\,\varphi(\boldsymbol{x}_{K,j},\cdot)\,\Big|\,\nabla\zeta\Big)_{0,Y_\eta(\boldsymbol{x}_{K,j})} = 0, \qquad \forall \zeta \in H^1_{\text{per}}\big(Y_\eta(\boldsymbol{x}_{K,j})\big), \end{cases} \tag{19}$$

with

$$\varphi_{H,\text{lin}}(\boldsymbol{x}) := \boldsymbol{v}_H(\boldsymbol{x}_{K,j})\cdot(\boldsymbol{x}-\boldsymbol{x}_{K,j}). \tag{20}$$

Similarly for $\boldsymbol{w}_H \in \boldsymbol{V}_{H,0}$*, let the function* ψ *be given in the same way replacing* $\boldsymbol{v}_H$ *with* $\boldsymbol{w}_H$ *in* (19)–(20)*. Then it holds*

$$(\varepsilon^{\text{eff}}\boldsymbol{v}_H\,|\,\boldsymbol{w}_H)_H = \sum_{K\in\mathcal{T}_H}\sum_{j=1}^{J_K}\frac{\omega_{K,j}}{|Y_\eta|}\Big(\varepsilon\Big(\boldsymbol{x}_{K,j},\frac{\cdot}{\eta}\Big)\nabla_{\boldsymbol{y}}\,\varphi(\boldsymbol{x}_{K,j},\cdot)\,\Big|\,\nabla_{\boldsymbol{y}}\,\psi(\boldsymbol{x}_{K,j},\cdot)\Big)_{0,Y_\eta(\boldsymbol{x}_{K,j})}.$$

The proof of Lemma 9 is very similar to the one of Lemma 8 and, more classically, to the proof of the reformulation of the HMM bilinear form, see e.g. [26]. Similar to (18) the solution of the micro problem can be written as

$$\varphi(\boldsymbol{x}_{K,j},\boldsymbol{x}) = \varphi_{H,\text{lin}}(\boldsymbol{x}) + \eta\sum_{k=1}^{3}\chi_k^\varepsilon\Big(\boldsymbol{x}_{K,j},\frac{\boldsymbol{x}-\boldsymbol{x}_{K,j}}{\eta}\Big)\big(\boldsymbol{v}_H(\boldsymbol{x}_{K,j})\big)_k, \tag{21}$$

with χ_k^ε defined in (6).

Remark 6. Here, we use only one property from $\varphi_{H,\text{lin}}$ in the proof, namely

$$\nabla\,\varphi_{H,\text{lin}}(\boldsymbol{x}) = \boldsymbol{v}_H(\boldsymbol{x}_{K,j}) \qquad \text{for all } \boldsymbol{x}\in Y_\eta(\boldsymbol{x}_{K,j})$$

and every other function having this property could be used as well.

3.2. Microscale solvers

Numerically, the micro solvers are closely related to the reformulated cell problem (12)–(13) and (19)–(20). In fact, they are their discretized versions with suitable finite element spaces. Therefore, we consider a family of shape regular tetrahedral meshes $\big(\mathcal{T}_h(\boldsymbol{x}_{K,j})\big)_h$ of the sampling domains $Y_\eta(\boldsymbol{x}_{K,j})$. For these meshes the mesh size h must resolve all the micro scale details of the material. Nevertheless, this does not lead to restrictive computational costs, because the sampling domains are small since they scale like η.

To approximate the effective permittivity we define discrete subspaces of $H^1_{\mathrm{per}}\big(Y_\eta(\boldsymbol{x}_{K,j})\big)$ based on Lagrange finite elements with periodic boundary conditions $W^k_{h,\mathrm{per}}$, where $k \in \mathbb{N}_0$ denotes the order of the finite element. The micro solvers corresponding to the electric permittivity centered at $\boldsymbol{x}_{K,j}$ and constrained by $\boldsymbol{v}_H \in \boldsymbol{V}_{H,0}$ are given by

$$\begin{cases} \text{Find } \varphi_h(\boldsymbol{x}_{K,j},\cdot) \in \varphi_{H,\mathrm{lin}} + W^k_{h,\mathrm{per}}, \text{ such that } \displaystyle\int_{Y_\eta(\boldsymbol{x}_{K,j})} \varphi_h(\boldsymbol{x}_{K,j},\boldsymbol{x})\,dx = 0 \text{ and} \\ \left(\varepsilon\Big(\boldsymbol{x}_{K,j},\dfrac{\cdot}{\eta}\Big)\,\nabla_{\boldsymbol{y}}\,\varphi_h(\boldsymbol{x}_{K,j},\cdot)\,\middle|\,\nabla\,\zeta_h\right)_{0,Y_\eta(\boldsymbol{x}_{K,j})} = 0, \qquad \forall \zeta_h \in W^k_{h,\mathrm{per}}. \end{cases} \tag{22}$$

To characterize φ_h, one must discretize the constraint (20). At the discrete level and because $\varphi_{H,\mathrm{lin}}$ defined by (20) is linear, the coupling constraint to $\boldsymbol{v}_H$ is discretized exactly.

Remark 7. In Section 2.2 we noticed that the cell problem (6) belonging to the computation of the effective electric permittivity is the usual cell problem, well-known in the homogenization theory of elliptic problems. Hence, this micro solver is closely related to the micro solver of standard FE-HMM schemes and the micro solver for the permittivity proposed in [17].

To approximate the effective inverse permeability the corresponding micro solver is more involved for two reasons. On one hand, the micro problem is vector-valued and involves the **curl**-operator. Thus, we use an edge element space $\boldsymbol{V}^k_{h,\mathrm{per}}$ with order k finite elements, where k is the same as above, with periodic boundary conditions, defined over the same mesh $\mathcal{T}_h(\boldsymbol{x}_{K,j})$ (see e.g. [27] for a definition of the basis functions). On the other hand, we use a mixed formulation [28, Sec. 3]. The micro solvers corresponding to the magnetic permeability centered at $\boldsymbol{x}_{K,j}$ and constrained by $\boldsymbol{v}_H \in \boldsymbol{V}_{H,0}$ is given by

$$\begin{cases} \text{Find } \big(\boldsymbol{v}_h(\boldsymbol{x}_{K,j},\cdot), p_h\big) \in \big(\boldsymbol{v}_{H,\mathrm{lin}} + \boldsymbol{V}^k_{h,\mathrm{per}}\big) \times W^k_{h,\mathrm{per}}, \\ \text{such that } \displaystyle\int_{Y_\eta(\boldsymbol{x}_{K,j})} \boldsymbol{v}_h(\boldsymbol{x}_{K,j},\boldsymbol{x})\,d\boldsymbol{x} = \boldsymbol{0},\ \int_{Y_\eta(\boldsymbol{x}_{K,j})} p_h(\boldsymbol{x})\,d\boldsymbol{x} = 0, \text{ and} \\ \left(\nu\Big(\boldsymbol{x}_{K,j},\dfrac{\cdot}{\eta}\Big)\,\mathbf{curl}_{\boldsymbol{y}}\,\boldsymbol{v}_h(\boldsymbol{x}_{K,j},\cdot)\,\middle|\,\mathbf{curl}\,\boldsymbol{\zeta}_h\right)_{0,Y_\eta(\boldsymbol{x}_{K,j})} + \\ \qquad\qquad \left(\boldsymbol{v}_h(\boldsymbol{x}_{K,j},\cdot)\,\middle|\,\nabla\,q_h\right)_{0,Y_\eta(\boldsymbol{x}_{K,j})} + \left(\boldsymbol{\zeta}_h\,\middle|\,\nabla\,p_h\right)_{0,Y_\eta(\boldsymbol{x}_{K,j})} = 0, \\ \text{for all } (\boldsymbol{\zeta}_h, q_h) \in \boldsymbol{V}^k_{h,\mathrm{per}} \times W^k_{h,\mathrm{per}}. \end{cases} \tag{23}$$

To characterize $\boldsymbol{v}_h$, one must also discretize (13). At the discrete level and because $\boldsymbol{v}_{H,\mathrm{lin}}$ defined by (13) belongs to $\boldsymbol{V}^k_h$, the coupling to $\boldsymbol{v}_H$ is discretized exactly. Note, that because $\nabla W^k_{h,\mathrm{per}} \subset \boldsymbol{V}^k_{h,\mathrm{per}}$, the discrete Lagrange multiplier p_h vanishes.

Remark 8. The condition on the vanishing mean in (22) and (23) can be implemented by introducing Lagrange multipliers. A detailed description of this procedure can be found in [29, Sec. 3.2].

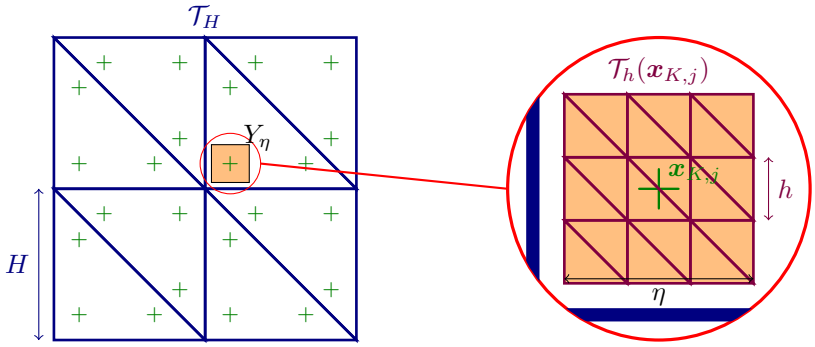

Figure 1: Two-dimensional sketch of the FE-HMM algorithm.

3.3. FE-HMM algorithm

Having now introduced all ingredients, let us present our FE-HMM scheme to approximate the effective behavior of (1).

$$\begin{cases} \text{Find } \boldsymbol{e}_H^{\mathrm{HMM}} \in \boldsymbol{V}_{H,0}, \text{ such that} \\ B_H^{\mathrm{HMM}}(\boldsymbol{e}_H^{\mathrm{HMM}} \,|\, \boldsymbol{v}_H) - \omega^2 (\boldsymbol{e}_H^{\mathrm{HMM}} \,|\, \boldsymbol{w}_H)_H^{\mathrm{HMM}} = (\boldsymbol{f} \,|\, \boldsymbol{v}_H)_{0,\Omega}, \qquad \forall \boldsymbol{v}_H \in \boldsymbol{V}_{H,0}, \end{cases} \tag{24}$$

with

$$B_H^{\mathrm{HMM}}(\boldsymbol{v}_H \,|\, \boldsymbol{w}_H) := \sum_{K,j} \frac{\omega_{K,j}}{|Y_\eta|} \left(\nu\Big(\boldsymbol{x}_{K,j}, \frac{\cdot}{\eta}\Big)\, \mathbf{curl}_{\boldsymbol{y}}\, \boldsymbol{v}_h(\boldsymbol{x}_{K,j}, \cdot) \,\middle|\, \mathbf{curl}_{\boldsymbol{y}}\, \boldsymbol{w}_h(\boldsymbol{x}_{K,j}, \cdot) \right)_{0, Y_\eta(\boldsymbol{x}_{K,j})},$$

$$(\boldsymbol{v}_H \,|\, \boldsymbol{w}_H)_H^{\mathrm{HMM}} := \sum_{K,j} \frac{\omega_{K,j}}{|Y_\eta|} \left(\varepsilon\Big(\boldsymbol{x}_{K,j}, \frac{\cdot}{\eta}\Big)\, \nabla_{\boldsymbol{y}}\, \varphi_h(\boldsymbol{x}_{K,j}, \cdot) \,\middle|\, \nabla_{\boldsymbol{y}}\, \psi_h(\boldsymbol{x}_{K,j}, \cdot) \right)_{0, Y_\eta(\boldsymbol{x}_{K,j})},$$

for all $\boldsymbol{v}_H, \boldsymbol{w}_H \in \boldsymbol{V}_{H,0}$, where $\boldsymbol{v}_h$ and φ_h (respectively $\boldsymbol{w}_h$ and ψ_h) are the solutions of the micro solvers (23) and (22) constrained by $\boldsymbol{v}_H$ (respectively $\boldsymbol{w}_H$). The summation should be taken over all $K \in \mathcal{T}_H$ and over all $j = 1, \ldots, J_K$. A two-dimensional illustration of the algorithm can be found in Figure 1. On its left, the computational domain triangulated with a macroscopic simplicial mesh $\mathcal{T}_H$ is shown in blue. The green crosses represent the nodes $\boldsymbol{x}_{K,j}$ of the quadrature formula that must be chosen in every macroscopic element K. Around each quadrature node we use two micro solvers in the microscopic sampling domains $Y_\eta(\boldsymbol{x}_{K,j})$. For this numerical solution the sampling domains are triangulated with a microscopic mesh $\mathcal{T}_h(\boldsymbol{x}_{K,j})$. In the right of Figure 1 only one such sampling domain is depicted in orange with a zoom of it, where the microscopic mesh is shown in violet.

4. A priori error analysis

In this section we prove our main result, an a priori error bound of the FE-HMM scheme presented above. But before, we recall the notion of T_H-coercivity, the essential tool in our error analysis. As the name suggests, T_H-coercivity is the counterpart of

T-coercivity already mentioned in Section 2 for discretized problems. We repeat its definition from [19] adapted to our setting.

Definition 5. A family of bilinear forms $(\mathfrak{B}_H)_H$ is *uniformly T_H-coercive* if there exist $\alpha^*, \beta^* > 0$ such that for all $H > 0$ there is an isomorphism $T_H \in \mathcal{L}(\boldsymbol{V}_{H,0})$ with

$$\big|\mathfrak{B}_H(\boldsymbol{v}_H, T_H\boldsymbol{v}_H)\big| \geq \alpha^* \|\boldsymbol{v}_H\|^2_{\mathbf{curl},\Omega}, \quad \forall \boldsymbol{v}_H \in \boldsymbol{V}_{H,0} \qquad \text{and} \qquad \big|\!\big|\!\big|T_H\big|\!\big|\!\big| \leq \beta^*.$$

If the discretized T_H-coercive bilinear form $\mathfrak{B}_H$ converges to the T-coercive bilinear form $\mathfrak{B}$, then we have an abstract a priori error for the corresponding Galerkin approximation.

Theorem 10 (cf. [19, Thm. 2]). *Let $\mathfrak{B}$ be a T-coercive bilinear form in $\boldsymbol{H}_0(\boldsymbol{curl};\Omega)$ and $\boldsymbol{u}$ be the solution to*

$$\begin{cases} \text{Find } \boldsymbol{u} \in \boldsymbol{H}_0(\boldsymbol{curl};\Omega), \text{ such that} \\ \mathfrak{B}(\boldsymbol{u} \,|\, \boldsymbol{v}) = (\boldsymbol{f} \,|\, \boldsymbol{v})_{0,\Omega}, \qquad \text{for all } \boldsymbol{v} \in \boldsymbol{H}_0(\boldsymbol{curl};\Omega). \end{cases}$$

If the family of bilinear forms $(\mathfrak{B}_H)_H$ is uniformly bounded and uniformly T_H-coercive, then the discretized problems

$$\begin{cases} \text{Find } \boldsymbol{u}_H \in \boldsymbol{V}_{H,0}, \text{ such that} \\ \mathfrak{B}_H(\boldsymbol{u}_H \,|\, \boldsymbol{v}_H) = (\boldsymbol{f} \,|\, \boldsymbol{v}_H)_{0,\Omega}, \qquad \text{for all } \boldsymbol{v}_H \in \boldsymbol{V}_{H,0}, \end{cases} \tag{25}$$

are well-posed and the following error bound holds with $C > 0$ independent of H

$$\big\|\boldsymbol{u} - \boldsymbol{u}_H\big\|_{\boldsymbol{curl},\Omega} \leq C \inf_{\boldsymbol{v}_H \in \boldsymbol{V}_{H,0}} \Big(\big\|\boldsymbol{u} - \boldsymbol{v}_H\big\|_{\boldsymbol{curl},\Omega} + \mathrm{Cons}_{\mathfrak{B},\mathfrak{B}_H}(\boldsymbol{v}_H) \Big).$$

The consistency term is given by

$$\mathrm{Cons}_{\mathfrak{B},\mathfrak{B}_H}(\boldsymbol{v}_H) = \sup_{\substack{\boldsymbol{w}_H \in \boldsymbol{V}_{H,0} \\ \boldsymbol{w}_H \neq 0}} \frac{\big|\mathfrak{B}(\boldsymbol{v}_H \,|\, \boldsymbol{w}_H) - \mathfrak{B}_H(\boldsymbol{v}_H \,|\, \boldsymbol{w}_H)\big|}{\|\boldsymbol{w}_H\|_{\boldsymbol{curl},\Omega}}.$$

Remark 9. Let $(\tilde{\mathfrak{B}}_H)_H$ be a second family of bilinear forms that is T_H-coercive for the same ismorphisms T_H and let $\tilde{\boldsymbol{u}}_H$ the solution of (25), where $\mathfrak{B}_H$ has been replaced by $\tilde{\mathfrak{B}}_H$, then

$$\big\|\tilde{\boldsymbol{u}}_H - \boldsymbol{u}_H\big\|_{\mathbf{curl},\Omega} \leq C\, \mathrm{Cons}_{\mathfrak{B}_H,\tilde{\mathfrak{B}}_H}(\boldsymbol{u}_H).$$

To prove an a priori error bound of our FE-HMM scheme, we will split the error as follows

$$\big\|\boldsymbol{e}^{\mathrm{eff}} - \boldsymbol{e}_H^{\mathrm{HMM}}\big\|_{\mathbf{curl},\Omega} \leq \big\|\boldsymbol{e}^{\mathrm{eff}} - \boldsymbol{e}_H^{\mathrm{eff}}\big\|_{\mathbf{curl},\Omega} + \big\|\boldsymbol{e}_H^{\mathrm{eff}} - \boldsymbol{e}_H^{\mathrm{HMM}}\big\|_{\mathbf{curl},\Omega},$$

where $\boldsymbol{e}_H^{\mathrm{eff}}$ is the solution of the discretized effective equation

$$\begin{cases} \text{Find } \boldsymbol{e}_H^{\mathrm{eff}} \in \boldsymbol{V}_{H,0}, \text{ such that} \\ B^{\mathrm{eff}}(\boldsymbol{e}_H^{\mathrm{eff}} \,|\, \boldsymbol{v}_H) - \omega^2 (\varepsilon^{\mathrm{eff}} \boldsymbol{e}_H^{\mathrm{eff}} \,|\, \boldsymbol{v}_H)_H = (\boldsymbol{f} \,|\, \boldsymbol{v}_H)_{0,\Omega}, \qquad \forall \boldsymbol{v}_H \in \boldsymbol{V}_{H,0}. \end{cases}$$

To simplify the notation we introduce the macro and HMM errors

$$\begin{aligned}
\mathrm{err}^{\nu}_{\mathrm{mac}} &:= \sup_{\substack{\boldsymbol{v}_H,\boldsymbol{w}_H\in\boldsymbol{V}_{H,0}\\ \boldsymbol{v}_H,\boldsymbol{w}_H\neq\boldsymbol{0}}} \frac{\big|(\nu^{\mathrm{eff}}\,\mathbf{curl}\,\boldsymbol{v}_H\,|\,\mathbf{curl}\,\boldsymbol{w}_H)_{0,\Omega} - B_H^{\mathrm{eff}}(\boldsymbol{v}_H\,|\,\boldsymbol{w}_H)\big|}{\|\boldsymbol{v}_H\|_{\mathbf{curl},\Omega}\|\boldsymbol{w}_H\|_{\mathbf{curl},\Omega}},\\
\mathrm{err}^{\nu}_{\mathrm{HMM}} &:= \sup_{\substack{\boldsymbol{v}_H,\boldsymbol{w}_H\in\boldsymbol{V}_{H,0}\\ \boldsymbol{v}_H,\boldsymbol{w}_H\neq\boldsymbol{0}}} \frac{\big|B_H^{\mathrm{eff}}(\boldsymbol{v}_H\,|\,\boldsymbol{w}_H) - B_H^{\mathrm{HMM}}(\boldsymbol{v}_H\,|\,\boldsymbol{w}_H)\big|}{\|\boldsymbol{v}_H\|_{\mathbf{curl},\Omega}\|\boldsymbol{w}_H\|_{\mathbf{curl},\Omega}},\\
\mathrm{err}^{\varepsilon}_{\mathrm{mac}} &:= \sup_{\substack{\boldsymbol{v}_H,\boldsymbol{w}_H\in\boldsymbol{V}_{H,0}\\ \boldsymbol{v}_H,\boldsymbol{w}_H\neq\boldsymbol{0}}} \frac{\big|(\varepsilon^{\mathrm{eff}}\boldsymbol{v}_H\,|\,\boldsymbol{w}_H)_{0,\Omega} - (\varepsilon^{\mathrm{eff}}\boldsymbol{v}_H\,|\,\boldsymbol{w}_H)_H\big|}{\|\boldsymbol{v}_H\|_{\mathbf{curl},\Omega}\|\boldsymbol{w}_H\|_{\mathbf{curl},\Omega}},\\
\mathrm{err}^{\varepsilon}_{\mathrm{HMM}} &:= \sup_{\substack{\boldsymbol{v}_H,\boldsymbol{w}_H\in\boldsymbol{V}_{H,0}\\ \boldsymbol{v}_H,\boldsymbol{w}_H\neq\boldsymbol{0}}} \frac{\big|(\varepsilon^{\mathrm{eff}}\boldsymbol{v}_H\,|\,\boldsymbol{w}_H)_H - (\boldsymbol{v}_H\,|\,\boldsymbol{w}_H)_H^{\mathrm{HMM}}\big|}{\|\boldsymbol{v}_H\|_{\mathbf{curl},\Omega}\|\boldsymbol{w}_H\|_{\mathbf{curl},\Omega}}.
\end{aligned}$$

Remark 10. These error terms are nothing else than differences of bilinear forms in the corresponding norm $|||\cdot|||$ over $\boldsymbol{V}_{H,0}$. E.g. we have $\mathrm{err}^{\nu}_{\mathrm{HMM}} = |||B_H^{\mathrm{eff}} - B_H^{\mathrm{HMM}}|||$.

With this notation, we can now state our main result.

Theorem 11. *Let the assumptions* (A_1)*–*(A_3) *be fullfilled. Assume further that*

$$\mathrm{err}^{\varepsilon}_{\mathrm{mac}}, \mathrm{err}^{\nu}_{\mathrm{mac}} \to 0 \qquad \text{as } H \to 0 \tag{Q}$$

and

$$\mathrm{err}^{\varepsilon}_{\mathrm{HMM}}, \mathrm{err}^{\nu}_{\mathrm{HMM}} \to 0 \qquad \text{as } h \to 0. \tag{R}$$

Then, the solution $\boldsymbol{e}_H^{\mathrm{HMM}}$ *of the FE-HMM scheme* (24) *converges to the solution* $\boldsymbol{e}^{\mathrm{eff}}$ *of the effective Maxwell's equations* (8) *as* H *and* h *tend to* 0*. Furthermore, for* H *and* h *small enough the following error estimates holds*

$$\begin{aligned}
\big\|\boldsymbol{e}^{\mathrm{eff}} - \boldsymbol{e}_H^{\mathrm{HMM}}\big\|_{\boldsymbol{curl},\Omega} \le C \inf_{\boldsymbol{v}_H\in\boldsymbol{V}_{H,0}} \Big(\big\|\boldsymbol{e}^{\mathrm{eff}} - \boldsymbol{v}_H\big\|_{\boldsymbol{curl},\Omega} + \big(\mathrm{err}^{\nu}_{\mathrm{mac}} + \omega^2 \mathrm{err}^{\varepsilon}_{\mathrm{mac}}\big)\|\boldsymbol{v}_H\|_{\boldsymbol{curl},\Omega} \Big)\\
+ C\big(\mathrm{err}^{\nu}_{\mathrm{HMM}} + \omega^2 \mathrm{err}^{\varepsilon}_{\mathrm{HMM}}\big)\|\boldsymbol{e}_H^{\mathrm{eff}}\|_{\boldsymbol{curl},\Omega}.
\end{aligned} \tag{26}$$

Proof. According to Theorem 7 the effective equation (8) is well-posed. Thus $\mathfrak{B}^{\mathrm{eff}}$ is T-coercive [19, Thm. 1]. This means that there exists a bijection $T^{\mathrm{eff}} : \boldsymbol{H}_0(\mathbf{curl};\Omega) \to \boldsymbol{H}_0(\mathbf{curl};\Omega)$ and $\alpha^{\mathrm{eff}} > 0$ such that

$$\mathfrak{B}^{\mathrm{eff}}(\boldsymbol{v}\,|\,T^{\mathrm{eff}}\boldsymbol{v}) \ge \alpha^{\mathrm{eff}}\|\boldsymbol{v}\|^2_{\mathbf{curl},\Omega}.$$

Furthermore, we can follow [19, Sec. 4.2] to explicitely define T^{eff}. We choose $(T_H)_H$ to be the family of isomorphisms approximating T^{eff} given as in [19, Sec. 4.3]. We now have

to show that $\mathfrak{B}_H^{\mathrm{eff}}$ and $\mathfrak{B}_H^{\mathrm{HMM}}$ are both T_H-coercive with these specific isomorphisms. Using the triangular inequality we find

$$\begin{aligned}
&\big|\mathfrak{B}_H^{\mathrm{eff}}(\boldsymbol{v}_H \,|\, T_H\boldsymbol{v}_H)\big| \\
&\quad \geq \big|\mathfrak{B}^{\mathrm{eff}}(\boldsymbol{v}_H \,|\, T^{\mathrm{eff}}\boldsymbol{v}_H)\big| - \big|\mathfrak{B}^{\mathrm{eff}}(\boldsymbol{v}_H \,|\, (T^{\mathrm{eff}} - T_H)\boldsymbol{v}_H)\big| - \Big|\big(\mathfrak{B}^{\mathrm{eff}} - \mathfrak{B}_H^{\mathrm{eff}}\big)\big(\boldsymbol{v}_H \,\big|\, T_H\boldsymbol{v}_H\big)\Big| \\
&\quad \geq \Big(\alpha^{\mathrm{eff}} - |||\mathfrak{B}^{\mathrm{eff}}||| \, |||T^{\mathrm{eff}} - T_H||| - |||\mathfrak{B}^{\mathrm{eff}} - \mathfrak{B}_H^{\mathrm{eff}}||| \, |||T_H|||\Big)\|\boldsymbol{v}_H\|^2_{\mathbf{curl},\Omega},
\end{aligned}$$

where we used in the second inequality the T^{eff}-coercivity of $\mathfrak{B}^{\mathrm{eff}}$. From [19] we know that $|||T_H|||$ is bounded and $|||T^{\mathrm{eff}} - T_H||| \to 0$ as $H \to 0$. Because of (A_2) $|||B^{\mathrm{eff}}|||$ is bounded as well. Due to the definition of the macro error, we have

$$|||\mathfrak{B}^{\mathrm{eff}} - \mathfrak{B}_H^{\mathrm{eff}}||| \leq \mathrm{err}_{\mathrm{mac}}^{\nu} + \omega^2 \mathrm{err}_{\mathrm{mac}}^{\varepsilon}.$$

and the macro errors converge to 0 as $H \to 0$ because of the assumptions (Q). Hence, for all $0 < \alpha^* < \alpha^{\mathrm{eff}}$ there is a threshold value $\tilde{H} > 0$ such that

$$\big|\mathfrak{B}_H^{\mathrm{eff}}(\boldsymbol{v}_H \,|\, T_H\boldsymbol{v}_H)\big| \geq \alpha^* \|\boldsymbol{v}_H\|^2_{\mathbf{curl},\Omega}$$

for all $H \leq \tilde{H}$. This shows the T_H-coercivity of $\mathfrak{B}_H^{\mathrm{eff}}$. For $\mathfrak{B}_H^{\mathrm{HMM}}$ we can proceed in the same way. We find

$$|||\mathfrak{B}^{\mathrm{eff}} - \mathfrak{B}_H^{\mathrm{HMM}}||| \leq \mathrm{err}_{\mathrm{mac}}^{\nu} + \mathrm{err}_{\mathrm{HMM}}^{\nu} + \omega^2\big(\mathrm{err}_{\mathrm{mac}}^{\varepsilon} + \mathrm{err}_{\mathrm{HMM}}^{\varepsilon}\big).$$

Hence we need not only assumption (Q) but also assumption (R), to show that $\mathfrak{B}_H^{\mathrm{HMM}}$ is T_H-coercive for H and h small enough.

As already mentioned we use the error splitting

$$\big\|\boldsymbol{e}^{\mathrm{eff}} - \boldsymbol{e}_H^{\mathrm{HMM}}\big\|_{\mathbf{curl},\Omega} \leq \big\|\boldsymbol{e}^{\mathrm{eff}} - \boldsymbol{e}_H^{\mathrm{eff}}\big\|_{\mathbf{curl},\Omega} + \big\|\boldsymbol{e}_H^{\mathrm{eff}} - \boldsymbol{e}_H^{\mathrm{HMM}}\big\|_{\mathbf{curl},\Omega}.$$

The first term can be estimated using Theorem 10 with $\boldsymbol{u} = \boldsymbol{e}^{\mathrm{eff}}$ and $\mathfrak{B} = \mathfrak{B}^{\mathrm{eff}}$ given by

$$\mathfrak{B}^{\mathrm{eff}}(\boldsymbol{v} \,|\, \boldsymbol{w}) = \big(\nu^{\mathrm{eff}}\,\mathbf{curl}\,\boldsymbol{v} \,\big|\, \mathbf{curl}\,\boldsymbol{w}\big)_{0,\Omega} - \omega^2\big(\varepsilon^{\mathrm{eff}}\boldsymbol{v} \,\big|\, \boldsymbol{w}\big)_{0,\Omega}, \quad \forall \boldsymbol{v}, \boldsymbol{w} \in \boldsymbol{H}_0(\mathbf{curl};\Omega)$$

and $\mathfrak{B}_H = \mathfrak{B}_H^{\mathrm{eff}}$ given by

$$\mathfrak{B}_H^{\mathrm{eff}}(\boldsymbol{v}_H \,|\, \boldsymbol{w}_H) = B_H^{\mathrm{eff}}(\boldsymbol{v}_H \,|\, \boldsymbol{w}_H) - \omega^2(\varepsilon^{\mathrm{eff}}\boldsymbol{v}_H \,|\, \boldsymbol{w}_H)_H, \qquad \forall \boldsymbol{v}_H, \boldsymbol{w}_H \in \boldsymbol{V}_{H,0}.$$

For the second term we will use Remark 9, with $\tilde{\mathfrak{B}}_H = \mathfrak{B}_H^{\mathrm{HMM}}$ given by

$$\mathfrak{B}_H^{\mathrm{HMM}}(\boldsymbol{v}_H \,|\, \boldsymbol{w}_H) = B_H^{\mathrm{HMM}}(\boldsymbol{v}_H \,|\, \boldsymbol{w}_H) - \omega^2(\boldsymbol{v}_H \,|\, \boldsymbol{w}_H)_H^{\mathrm{HMM}}, \qquad \forall \boldsymbol{v}_H, \boldsymbol{w}_H \in \boldsymbol{V}_{H,0}.$$

It is easy to see that the emerging consistency terms can be bounded as

$$\begin{aligned}
\mathrm{Cons}_{\mathfrak{B}^{\mathrm{eff}},\mathfrak{B}_H^{\mathrm{eff}}}(\boldsymbol{v}_H) &\leq (\mathrm{err}_{\mathrm{mac}}^{\nu} + \omega^2 \mathrm{err}_{\mathrm{mac}}^{\varepsilon})\|\boldsymbol{v}_H\|_{\mathbf{curl},\Omega}, \\
\mathrm{Cons}_{\mathfrak{B}^{\mathrm{eff}},\mathfrak{B}_H^{\mathrm{HMM}}}(\boldsymbol{e}_H^{\mathrm{eff}}) &\leq (\mathrm{err}_{\mathrm{HMM}}^{\nu} + \omega^2 \mathrm{err}_{\mathrm{HMM}}^{\varepsilon})\|\boldsymbol{e}_H^{\mathrm{eff}}\|_{\mathbf{curl},\Omega},
\end{aligned}$$

which finishes the proof. □

We see, that (Q) is correlated with the macro solver and (R) with the micro solver. In the next section, we give an example of a concrete setting, where both assumptions hold. We also illustrate there what can happen when one assumption is not fulfilled.

5. Practical illustrations

We consider now the assumptions (Q) and (R). More specifically, we describe settings in which the assumptions are satisfied. These settings are not exhaustive and our FE-HMM can be applied to other situations. A detailed study on the optimal assumptions such that assumptions (Q) and (R) are beyond the scope of this article. In this section, we always assume that the assumptions (A_1)–(A_2) hold. Furthermore, to have a specific instance of our FE-HMM scheme, we consider only finite element of order one. In particular,

$$\boldsymbol{V}_{H,0} = \left\{\boldsymbol{v}_H \in \boldsymbol{H}_0(\mathbf{curl};\Omega) : \boldsymbol{v}_H|_K \in \boldsymbol{\mathcal{R}}^1(K),\ \forall K \in \mathcal{T}_H\right\},$$

where $\boldsymbol{\mathcal{R}}^1(K)$ is given by

$$\boldsymbol{\mathcal{R}}^1(K) = \left\{\boldsymbol{v} \in \boldsymbol{\mathcal{P}}^1(K) : \boldsymbol{v}(\boldsymbol{x}) = \boldsymbol{a} + \boldsymbol{b} \times \boldsymbol{x},\ \boldsymbol{a},\boldsymbol{b} \in \mathbb{R}^3\right\}$$

and $\boldsymbol{\mathcal{P}}^1(K)$ is the space of vector-valued polynomials of total degree not greater than one. For more details for these finite element spaces we refer to [27]. The space for the micro solver (23) centered at $\boldsymbol{x}_{K,j}$ is given similarly by

$$\boldsymbol{V}^1_{h,\mathrm{per}} = \left\{\boldsymbol{v}_h \in \boldsymbol{H}_{\mathrm{per}}(\mathbf{curl}; Y_\eta(\boldsymbol{x}_{K,j})) : \boldsymbol{v}_h|_k \in \boldsymbol{\mathcal{R}}^1(k),\ \forall k \in \mathcal{T}_h(Y_\eta(\boldsymbol{x}_{K,j})\right\}$$

and the space for the other micro solver (22) is given by

$$W^1_{h,\mathrm{per}} = \left\{\varphi_h \in H^1_{\mathrm{per}}(Y_\eta(\boldsymbol{x}_{K,j})) : \varphi_h|_k \in \mathcal{P}^1(k),\ \forall k \in \mathcal{T}_h(Y_\eta(\boldsymbol{x}_{K,j})\right\},$$

where $\mathcal{P}^1(k)$ is the space of scalar-valued polynomials of total degree not greater than one.

As we have seen, the choice of a well-suited quadrature formula for FE-HMM is crucial, cf. [30]. Firstly, the quadrature must be accurate enough, such that (Q) holds. The second goal is to minimize the number of quadrature nodes per element. This is preferable in view of computational costs since our multiscale scheme requires the numerical solution of two micro problems per quadrature node. With these two goals in mind, we choose the quadrature formula denoted by (QF_0) $(\hat{x}_j, \hat{w}_j)_{j=1}^4$ on the reference simplex $\hat{K}$ whose nodes and weights are given in Table 1. This quadrature formula is exact for the function space $\boldsymbol{\mathcal{P}}^2(\hat{K})$ and it is well known that there is no quadrature formula having this property with fewer nodes [31, Section 4.5]. Due to the affine mapping F_K from $\hat{K}$ to K a corresponding quadrature formula $(\boldsymbol{x}_{K,j}, \omega_{K,j})_{j=1}^4$ is given on every $K \in \mathcal{T}_H$ by

$$\boldsymbol{x}_{K,j} = F_K(\hat{\boldsymbol{x}}_j) \qquad \text{and} \qquad \omega_{K,j} = \det D(F_K)\hat{\omega}_j,$$

for $j = 1, \dots 4$, where $D(F_K)$ is the (constant) Jacobian of F_K. It is easy to see, that the property carries over, i.e. $(\boldsymbol{x}_{K,j}, \omega_{K,j})_{j=1}^4$ is exact for the space $\boldsymbol{\mathcal{P}}^2(K)$. Choosing the quadrature formula (QF_0), the number of quadrature nodes per elements J_K is equal to four for all $K \in \mathcal{T}_H$. This construction for the quadrature formula on K is the standard procedure for finite elements [32, Sec. 4.1].

We show now, that in this setting (Q) holds for periodic materials.

Table 1: Quadrature formula (QF_0) for the reference tetrahedron $\hat{K}$

j	node $\hat{x}_j$	weight $\hat{\omega}_j$
1	$\frac{1}{4}\left(1-\frac{1}{\sqrt{5}}, 1-\frac{1}{\sqrt{5}}, 1-\frac{1}{\sqrt{5}}\right)$	$\frac{1}{24}$
2	$\frac{1}{4}\left(1-\frac{1}{\sqrt{5}}, 1-\frac{1}{\sqrt{5}}, 1+\frac{3}{\sqrt{5}}\right)$	$\frac{1}{24}$
3	$\frac{1}{4}\left(1-\frac{1}{\sqrt{5}}, 1+\frac{3}{\sqrt{5}}, 1-\frac{1}{\sqrt{5}}\right)$	$\frac{1}{24}$
4	$\frac{1}{4}\left(1+\frac{3}{\sqrt{5}}, 1-\frac{1}{\sqrt{5}}, 1-\frac{1}{\sqrt{5}}\right)$	$\frac{1}{24}$

Lemma 12. *Let the permittivity and the inverse permeability be given by*

$$\varepsilon^\eta(\boldsymbol{x}) = \varepsilon\Big(\frac{\boldsymbol{x}}{\eta}\Big) \qquad \text{and} \qquad \nu^\eta(\boldsymbol{x}) = \nu\Big(\frac{\boldsymbol{x}}{\eta}\Big),$$

where $\varepsilon, \nu \in \big(L^\infty_{\mathrm{per}}(Y)\big)^{3\times 3}$ *are symmetric, uniformly coercive and bounded. Then, both macro errors* $\mathrm{err}^\varepsilon_{\mathrm{mac}}$ *and* $\mathrm{err}^\nu_{\mathrm{mac}}$ *vanish and the assumption* (Q) *holds for the above choices of the macro and micro finite element spaces and the quadrature formula* (QF_0).

Proof. From the definition of $\mathcal{H}$ and $\mathcal{K}$ it is easy to see, that $\varepsilon^{\mathrm{eff}}$ and ν^{eff} are constant on Ω for periodic materials and as a consequence

$$\varepsilon^{\mathrm{eff}}\boldsymbol{v}_H \cdot \boldsymbol{w}_H|_K \in \mathcal{P}^2(K), \qquad \nu^{\mathrm{eff}}\,\mathbf{curl}\,\boldsymbol{v}_H \cdot \mathbf{curl}\,\boldsymbol{w}_H|_K \in \mathcal{P}^0(K)$$

for all $\boldsymbol{v}_H, \boldsymbol{w}_H \in \boldsymbol{V}_{H,0}$ and all simplices K. Thus $(\varepsilon^{\mathrm{eff}}\boldsymbol{v}_H \,|\, \boldsymbol{w}_H)_{0,\Omega} = (\varepsilon^{\mathrm{eff}}\boldsymbol{v}_H \,|\, \boldsymbol{w}_H)_H$ and $B^{\mathrm{eff}}(\boldsymbol{v}_H \,|\, \boldsymbol{w}_H) = B^{\mathrm{eff}}_H(\boldsymbol{v}_H \,|\, \boldsymbol{w}_H)$. □

Remark 11. For local periodic material, the validity of (Q) can be shown under additional regularity assumptions on the effective permeability and permittivity tensors. If, e.g. $\varepsilon^{\mathrm{eff}}, \nu^{\mathrm{eff}} \in (C^1(\Omega))^{3\times 3}$, then the assumption (Q) holds for the above choices of the macro finite element space and the quadrature formula, although the macro errors do no longer necessarily vanish. This regularity condition is for example satisfied if the permittivity and the inverse permeability are given as in (3) with $\varepsilon, \nu \in \big(C^1(\Omega; W^{1,\infty}_{\mathrm{per}}(Y))\big)^{3\times 3}$. Then, $\varepsilon^{\mathrm{eff}} = \mathcal{H}(\varepsilon)$ and $\nu^{\mathrm{eff}} = \mathcal{K}(\nu)$ are in $(C^1(\Omega))^{3\times 3}$. Another possibility to fulfill the mentioned regularity assumption is to consider that the permittivity and the inverse permeability are again given as in (3) with

$$\varepsilon(\boldsymbol{x}, \boldsymbol{y}) = \varepsilon_{\boldsymbol{x}}(\boldsymbol{x})\varepsilon_{\boldsymbol{y}}(\boldsymbol{y})I_3 \qquad \text{and} \qquad \nu(\boldsymbol{x}, \boldsymbol{y}) = \nu_{\boldsymbol{x}}(\boldsymbol{x})\nu_{\boldsymbol{y}}(\boldsymbol{y})I_3,$$

with scalar functions $\varepsilon_{\boldsymbol{x}}, \nu_{\boldsymbol{x}} \in C^1(\Omega)$ and $\varepsilon_{\boldsymbol{y}}, \nu_{\boldsymbol{y}} \in \big(L^\infty_{\mathrm{per}}(Y)\big)^{3\times 3}$. The regularity follows, since in this case we have

$$\mathcal{H}(\varepsilon) = \varepsilon_{\boldsymbol{x}}\mathcal{H}(\varepsilon_{\boldsymbol{y}})I_3 \qquad \text{and} \qquad \mathcal{K}(\nu) = \nu_{\boldsymbol{x}}\mathcal{K}(\varepsilon_{\boldsymbol{y}})I_3.$$

To study the HMM errors we first recall the formulas (18) and (21) that we derived in the proofs of Lemma 8 and 9, respectively. There, the solution of the exact micro problems (12) and (19) are given as a linear combination of the solutions of cell problems (6) and (7) over the unit cell Y. We mimic this for the micro solvers. We first define a triangulation $\hat{\mathcal{T}}_{h/\eta}$ of Y corresponding to the triangulation of the sampling domain around $\boldsymbol{x}_{K,j}$ by

$$\hat{\mathcal{T}}_{h/\eta}(Y) := \frac{\mathcal{T}_h\big(Y_\eta(\boldsymbol{x}_{K,j})\big)}{\eta} - \boldsymbol{x}_{K,j}.$$

Note, that due to the scaling the new mesh size is h/η. Let $\hat{\boldsymbol{V}}_{h/\eta,\mathrm{per}}$ and $\hat{W}_{h/\eta,\mathrm{per}}$ be the corresponding spaces of first order edge elements and first order Lagrange finite elements, respectively, with periodic boundary conditions. Furthermore, let $\chi^{\varepsilon}_{k,h/\eta}(\boldsymbol{x}_{K,j},\cdot)$ be the finite element solution of (6) with $H^1_{\mathrm{per}}(Y)$ replaced by $\hat{W}_{h/\eta,\mathrm{per}}$. We find

$$\varphi_h(\boldsymbol{x}_{K,j},\boldsymbol{x}) = \varphi_{H,\mathrm{lin}}(\boldsymbol{x}) + \eta\sum_{k=1}^{3}\chi^{\varepsilon}_{k,h/\eta}\Big(\boldsymbol{x}_{K,j},\frac{\boldsymbol{x}-\boldsymbol{x}_{K,j}}{\eta}\Big)\big(\boldsymbol{v}_H(\boldsymbol{x}_{K,j})\big)_k \tag{27}$$

Similarly, let $\boldsymbol{\theta}^{\nu}_{k,h/\eta}(\boldsymbol{x}_{K,j},\cdot)$ be the finite element solution of (7) with $\boldsymbol{H}_{\mathrm{per}}(\mathbf{curl};Y)$ replaced by $\hat{\boldsymbol{V}}_{h/\eta,\mathrm{per}}$, such that we find

$$\begin{aligned}\boldsymbol{v}_h(\boldsymbol{x}_{K,j},\boldsymbol{x}) = \boldsymbol{v}_{H,\mathrm{lin}}(\boldsymbol{x}) - \frac{1}{|Y_\eta|}\int_{Y_\eta}\boldsymbol{v}_{H,\mathrm{lin}}(\boldsymbol{y})\,d\boldsymbol{y} + \\ \eta\sum_{k=1}^{3}\boldsymbol{\theta}^{\nu}_{k,h/\eta}\Big(\boldsymbol{x}_{K,j},\frac{\boldsymbol{x}-\boldsymbol{x}_{K,j}}{\eta}\Big)\big(\mathbf{curl}\,\boldsymbol{v}_H(\boldsymbol{x}_{K,j})\big)_k.\end{aligned} \tag{28}$$

The following lemma gives a sufficient condition to guarantee that the Assumption (R) holds.

Lemma 13 (HMM error). *Let the macro and micro finite element spaces and the quadrature formula be chosen as above.*

(i) *If there is $s^{\varepsilon} > 0$ such that $\nabla_{\boldsymbol{y}}\,\chi^{\varepsilon}_k(\boldsymbol{x}_{K,j},\cdot) \in \boldsymbol{H}^{s^{\varepsilon}}(Y)$ for $1 \le k \le 3$, then*

$$\mathrm{err}^{\varepsilon}_{\mathrm{HMM}} \le C\Big(\frac{h}{\eta}\Big)^{2s^{\varepsilon}}.$$

(ii) *If there is $s^{\nu} > 0$ such that $\boldsymbol{curl}_{\boldsymbol{y}}\,\boldsymbol{\theta}^{\nu}_k(\boldsymbol{x}_{K,j},\cdot) \in \boldsymbol{H}^{s^{\nu}}(Y)$ for $1 \le k \le 3$, then*

$$\mathrm{err}^{\nu}_{\mathrm{HMM}} \le C\Big(\frac{h}{\eta}\Big)^{2s^{\nu}}.$$

Furthermore, in (i)–(ii), the constant C is independent of h and η.

The proofs are similar to the proof of [26, Prop. 9, Lem. 10, and Prop. 14], where more detailed explanations can be found.

PROOF. *Ad* (i)*:* Owing to Lemma 9 it is easy to see that

$$\begin{aligned}
&\big|(\varepsilon^{\mathrm{eff}}\boldsymbol{v}_H \,|\, \boldsymbol{w}_H)_H - (\boldsymbol{v}_H \,|\, \boldsymbol{w}_H)_H^{\mathrm{HMM}}\big| \\
&\quad = \left|\sum_{K,j} \frac{\omega_{K,j}}{|Y_\eta(\boldsymbol{x}_{K,j})|} \int_{Y_\eta(\boldsymbol{x}_{K,j})} \varepsilon^\eta (\nabla_{\boldsymbol{y}}\,\varphi_h - \nabla_{\boldsymbol{y}}\,\varphi)\cdot(\nabla_{\boldsymbol{y}}\,\psi - \nabla_{\boldsymbol{y}}\,\psi_h)\,dx\right| \\
&\quad \le C\sum_{K,j} \frac{\omega_{K,j}}{|Y_\eta(\boldsymbol{x}_{K,j})|} \big\|\nabla_{\boldsymbol{y}}\,\varphi - \nabla_{\boldsymbol{y}}\,\varphi_h\big\|_{0,Y_\eta(\boldsymbol{x}_{K,j})} \big\|\nabla_{\boldsymbol{y}}\,\psi - \nabla_{\boldsymbol{y}}\,\psi_h\big\|_{0,Y_\eta(\boldsymbol{x}_{K,j})},
\end{aligned}$$

where we used the positivity of the weights and the boundedness of ε^η. With the help of formulas (21) and (27) find

$$\begin{aligned}
&\|\nabla_{\boldsymbol{y}}\,\varphi - \nabla_{\boldsymbol{y}}\,\varphi_h\|_{L^2(Y_\eta(\boldsymbol{x}_{K,j}))} \\
&\quad \le C\sqrt{|Y_\eta(\boldsymbol{x}_{K,j})|}\,\max_k \Big\|\nabla_{\boldsymbol{y}}\,\chi_k^\varepsilon - \nabla_{\boldsymbol{y}}\,\chi_{k,h/\eta}^\varepsilon\Big\|_{0,Y} |\boldsymbol{v}_H(\boldsymbol{x}_{K,j})|.
\end{aligned}$$

The difference between ψ and ψ_h can be bounded in the same way. Because of the assumed regularity standard convergence results for finite elements [33] yield

$$\|\nabla_{\boldsymbol{y}}\,\chi_k^\varepsilon(\boldsymbol{x}_{K,j},\cdot) - \nabla_{\boldsymbol{y}}\,\chi_{k,h/\eta}^\varepsilon(\boldsymbol{x}_{K,j},\cdot)\|_{0,Y} \le C\Big(\frac{h}{\eta}\Big)^{s^\varepsilon} \big\|\nabla_{\boldsymbol{y}}\,\chi_k^\varepsilon(\boldsymbol{x}_{K,j},\cdot)\big\|_{s^\varepsilon,Y},$$

where we can absorb $\|\nabla_{\boldsymbol{y}}\,\chi_k^\varepsilon\|_{s^\varepsilon,Y}$ in the constant, since it does not depend on η, H, or h. Combining these inequalities we get

$$\begin{aligned}
\Big|(\varepsilon^{\mathrm{eff}}\boldsymbol{v}_H \,|\, \boldsymbol{w}_H)_H - (\boldsymbol{v}_H \,|\, \boldsymbol{w}_H)_H^{\mathrm{HMM}}\Big| &\le C\Big(\frac{h}{\eta}\Big)^{2s^\varepsilon} \sum_{K,j} \omega_{K,j} \big|\boldsymbol{v}_H(\boldsymbol{x}_{K,j})\big|\,\big|\boldsymbol{w}_H(\boldsymbol{x}_{K,j})\big| \\
&\le C\Big(\frac{h}{\eta}\Big)^{2s^\varepsilon} \big\|\boldsymbol{v}_H\big\|_{0,\Omega}\,\big\|\boldsymbol{w}_H\big\|_{0,\Omega},
\end{aligned}$$

where we used once more the positivity of the weights, the Cauchy-Schwarz inequality, and the exactness property of the quadrature formula in the second inequality. The result follows directly from the definition of $\mathrm{err}_{\mathrm{HMM}}^\varepsilon$.

Ad (ii)*:* For the second part we can follow closely the lines of the first part. From Lemma 8 we get

$$\begin{aligned}
&\big|B_H^{\mathrm{eff}}(\boldsymbol{v}_H \,|\, \boldsymbol{w}_H) - B_H^{\mathrm{HMM}}(\boldsymbol{v}_H \,|\, \boldsymbol{w}_H)\big| \\
&\quad \le C\sum_{K,j} \frac{\omega_{K,j}}{|Y_\eta(\boldsymbol{x}_{K,j})|} \big\|\mathbf{curl}_{\boldsymbol{y}}\,\boldsymbol{v} - \mathbf{curl}_{\boldsymbol{y}}\,\boldsymbol{v}_h\big\|_{0,Y_\eta(\boldsymbol{x}_{K,j})} \big\|\mathbf{curl}_{\boldsymbol{y}}\,\boldsymbol{w} - \mathbf{curl}_{\boldsymbol{y}}\,\boldsymbol{w}_h\big\|_{0,Y_\eta(\boldsymbol{x}_{K,j})}.
\end{aligned}$$

The difference between $\mathbf{curl}\,\boldsymbol{v}$ and $\mathbf{curl}\,\boldsymbol{v}_h$ (respectively between $\mathbf{curl}\,\boldsymbol{w}$ and $\mathbf{curl}\,\boldsymbol{w}_h$), can be bounded using formulas (18) and (28). Combining this with convergence results for edge elements [34] yields

$$\|\mathbf{curl}_{\boldsymbol{y}}\,\boldsymbol{v} - \mathbf{curl}_{\boldsymbol{y}}\,\boldsymbol{v}_h\|_{0,Y_\eta(\boldsymbol{x}_{K,j})} \le C\sqrt{|Y_\eta(\boldsymbol{x}_{K,j})|}\,\Big(\frac{h}{\eta}\Big)^{s^\nu} |\mathbf{curl}\,\boldsymbol{v}_H(\boldsymbol{x}_{K,j})|,$$

from where the claim follows. □

Remark 12. The rate of convergence s^ε and s^ν depend on the regularity of the solutions of the cell problems. It can be guaranteed if the involved material tensor are sufficiently regular. E.g., if ε and ν are symmetric and given as in (3) with $\varepsilon_{m,n}(\boldsymbol{x}_{K,j},\cdot), \nu_{m,n}(\boldsymbol{x}_{K,j},\cdot) \in W^{1,\infty}_{\mathrm{per}}(Y)$ for all $\boldsymbol{x}_{K,j}$ and $1 \leq m,n \leq 3$, then Lemma 13 holds with $s^\varepsilon = s^\nu = 1$ [35].

Remark 13. The condition $\nabla_{\boldsymbol{y}}\, \chi^\varepsilon_k(\boldsymbol{x}_{K,j},\cdot) \in \boldsymbol{H}^{s^\varepsilon}(Y)$ is equivalent to $\chi^\varepsilon_k(\boldsymbol{x}_{K,j},\cdot) \in H^{1+s^\varepsilon}(Y)$. This is a standard assumption in a priori error analysis of FE-HMM algorithms, cf. [14, Ass. (**H2**)]. In contrast, while it follows from $\boldsymbol{\theta}^\nu_k(\boldsymbol{x}_{K,j},\cdot) \in \boldsymbol{H}^{1+s^\nu}(Y)$ that $\mathbf{curl}_{\boldsymbol{y}}\, \boldsymbol{\theta}^\nu_k(\boldsymbol{x}_{K,j},\cdot) \in \boldsymbol{H}^{s^\nu}(Y)$, the converse it not true.

6. Numerical Experiments

In this section we present some numerical experiments. These experiments corroborate the theoretical results of the previous two sections and show that our FE-HMM scheme can be applied to more general settings. All the experiments where implemented with `FreeFem++` [36].

6.1. Periodic medium

We consider the model problem (1) in the unit cube $\Omega = (0,1)^3$ and $\omega = 1$. The electric permittivity and the magnetic permeability tensors are given by $\varepsilon^\eta(\boldsymbol{x}) = \varepsilon(\boldsymbol{x}/\eta) I_3$ and $\nu^\eta(\boldsymbol{x}) = \nu(\boldsymbol{x}/\eta) I_3$ with $\eta = 2^{-8}$ with

$$\varepsilon(\boldsymbol{y}) = \frac{\prod_{k=1}^3 \sqrt{2} + \sin(2\pi y_k)}{2} \qquad \text{and} \qquad \nu(\boldsymbol{y}) = \frac{2}{\prod_{k=1}^3 \sqrt{2} + \sin(2\pi y_k)}.$$

For this specific tensors the exact effective permittivity and permeability can be analytically computed, see e.g. [4, Sec. 1.2]. We find $\varepsilon^{\mathrm{eff}}(\boldsymbol{x}) = \nu^{\mathrm{eff}}(\boldsymbol{x}) = I_3$. Then, for the (curl-free) right-hand side

$$\boldsymbol{f}(\boldsymbol{x}) = -\begin{pmatrix} \cos(\pi x_1)\sin(\pi x_2)\sin(\pi x_3) \\ \sin(\pi x_1)\cos(\pi x_2)\sin(\pi x_3) \\ \sin(\pi x_1)\sin(\pi x_2)\cos(\pi x_3) \end{pmatrix}$$

the exact effective electric field $\boldsymbol{e}^{\mathrm{eff}}$ is given by $\boldsymbol{e}^{\mathrm{eff}}(\boldsymbol{x}) = -\boldsymbol{f}(\boldsymbol{x})$.

We compute an approximation $\boldsymbol{e}_H^{\mathrm{HMM}}$ of $\boldsymbol{e}^{\mathrm{eff}}$ with the FE-HMM scheme (24). More specifically, we use the same instance of the FE-HMM as described in Section 5, i.e. first order finite elements for the macro and the micro solver and the quadrature formula (QF_0). Note that we are in the situation of Lemma 12, thus the macro errors $\mathrm{err}^\varepsilon_{\mathrm{mac}}$ and $\mathrm{err}^\nu_{\mathrm{mac}}$ vanish. By computing $\|\boldsymbol{e}_H^{\mathrm{eff}} - \boldsymbol{e}_H^{\mathrm{HMM}}\|_{\mathbf{curl},\Omega}$, we consider the HMM-error. In the proof of Theorem 11, we have shown that

$$\|\boldsymbol{e}_H^{\mathrm{eff}} - \boldsymbol{e}_H^{\mathrm{HMM}}\|_{\mathbf{curl},\Omega} \leq C\big(\mathrm{err}^\nu_{\mathrm{HMM}} + \omega^2 \mathrm{err}^\varepsilon_{\mathrm{HMM}}\big)\|\boldsymbol{e}_H^{\mathrm{eff}}\|_{\mathbf{curl},\Omega}.$$

Because ε and ν are smooth, we expect second order convergence in h for $\|\boldsymbol{e}_H^{\mathrm{eff}} - \boldsymbol{e}_H^{\mathrm{HMM}}\|_{\mathbf{curl},\Omega}$, cf. Remark 12. We observe this order of convergence numerically, as it can be seen on the left side of Figure 2.

Let us now consider now the total error $\|\boldsymbol{e}^{\mathrm{eff}} - \boldsymbol{e}_H^{\mathrm{HMM}}\|_{\mathbf{curl},\Omega}$. Since we use finite elements of order one for the macro solver with a smooth solution $\boldsymbol{e}^{\mathrm{eff}}$, we have

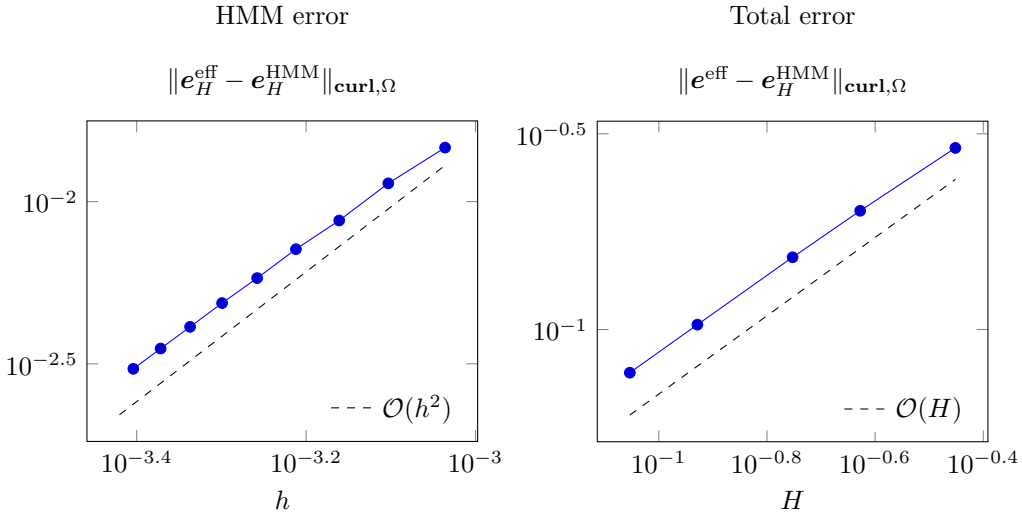

Figure 2: Left: error between the FEM solution of the effective Maxwell's equations $\boldsymbol{e}_H^{\text{eff}}$ and the corresponding FE-HMM solution $\boldsymbol{e}_H^{\text{HMM}}$ for different mesh sizes h of the micro solvers. The macro meshsize $H = \sqrt{2}/2$ is kept fixed for all h. Right: error between the exact effective solution $\boldsymbol{e}^{\text{eff}}$ and $\boldsymbol{e}_H^{\text{HMM}}$ for different mesh sizes H of the macro solver. The micro mesh size is refined simultaneously.

$\inf_{\boldsymbol{v}_H \in \boldsymbol{V}_{H,0}} \|\boldsymbol{e}^{\text{eff}} - \boldsymbol{v}_H\|_{\mathbf{curl},\Omega} \in \mathcal{O}(H)$. Hence we expect first order convergence in H due to (26). To get this convergence order, we can not simply fix the micro mesh size h, but need to refine it simultaneously. Since the consistency term $\text{Cons}_{\mathfrak{B}^{\text{eff}},\mathfrak{B}_H^{\text{HMM}}}$ scales like h^2, an appropriate refinement strategy consists in adapting the convergence order by ensuring that the ratio between H and h^2 does not change significantly. Doing so, we get the results depicted on the right side of Figure 2, where we retrieve the expected first order convergence of $\|\boldsymbol{e}^{\text{eff}} - \boldsymbol{e}_H^{\text{HMM}}\|_{\mathbf{curl},\Omega}$.

6.2. Stratified periodic medium

Again we consider the model problem (1), but we assume that the permittivity, the permeability, and the source term $\boldsymbol{f}$ are constant in x_3-direction. In this case $\boldsymbol{e}$ does not depend on x_3. If we assume in addition to (A_1)–(A_3) that the material tensors are given by

$$\varepsilon^\eta = \begin{pmatrix} \varepsilon_{11}^\eta & \varepsilon_{12}^\eta & 0 \\ \varepsilon_{21}^\eta & \varepsilon_{22}^\eta & 0 \\ 0 & 0 & \varepsilon_{33}^\eta \end{pmatrix}, \qquad \nu^\eta = \begin{pmatrix} \nu_{11}^\eta & \nu_{12}^\eta & 0 \\ \nu_{21}^\eta & \nu_{22}^\eta & 0 \\ 0 & 0 & \nu_{33}^\eta \end{pmatrix}$$

and that $\boldsymbol{f} = (f_1, f_2, 0)^T$, then there is no electric field in the x_3-direction (TE-mode). In this case (1) can be reduced to the two-dimensional problem

$$\begin{cases} \textit{Find } \boldsymbol{e}^\eta \in \boldsymbol{H}_0(\text{curl};\Omega) \textit{ such that} \\ (\tilde{\nu}^\eta \,\text{curl}\, \boldsymbol{e}^\eta \,|\, \text{curl}\, \boldsymbol{v})_{0,\Omega} - \omega^2 (\tilde{\varepsilon}^\eta \boldsymbol{e}^\eta \,|\, \boldsymbol{v})_{0,\Omega} = (\tilde{\boldsymbol{f}} \,|\, \boldsymbol{v})_{0,\Omega} \qquad \forall \boldsymbol{v} \in \boldsymbol{H}_0(\text{curl};\Omega), \end{cases}$$

with

$$\tilde{\varepsilon}^\eta = \begin{pmatrix} \varepsilon_{11}^\eta & \varepsilon_{12}^\eta \\ \varepsilon_{21}^\eta & \varepsilon_{22}^\eta \end{pmatrix}, \qquad \tilde{\nu}^\eta = \nu_{33}^\eta, \qquad \tilde{\boldsymbol{f}} = \begin{pmatrix} f_1 \\ f_2 \end{pmatrix}.$$

Table 2: Quadrature formula (QF_1) and (QF_2) for the reference triangle $\hat{K}$

	j	node $\hat{x}_j$	weight $\hat{\omega}_j$	Polynomial order
(QF_1)	1	$\frac{1}{5}(1,1)$	$\frac{1}{6}$	1
	2	$\frac{1}{5}(3,1)$	$\frac{1}{6}$	
	3	$\frac{1}{5}(1,3)$	$\frac{1}{6}$	
(QF_2)	1	$\frac{1}{6}(1,1)$	$\frac{1}{6}$	2
	2	$\frac{1}{6}(4,1)$	$\frac{1}{6}$	
	3	$\frac{1}{6}(1,4)$	$\frac{1}{6}$	

Here we use the scalar-valued curl given by $\operatorname{curl} \boldsymbol{v} = \partial_{x_1} v_2 - \partial_{x_2} v_1$. Note that the structure of the problem stays is the same as in the three-dimensional case. Thus, our FE-HMM scheme can be used here as well, without any conceptual modification.

First, we set $\Omega = (0,1)^2$, $\omega = 1$, and consider again a periodic medium with $\tilde{\varepsilon}^\eta(\boldsymbol{x}) = \varepsilon(\boldsymbol{x}/\eta) I_2$ and $\tilde{\nu}^\eta(\boldsymbol{x}) = \nu(\boldsymbol{x}/\eta)$, with $\eta = 2^{-8}$ and ε and ν defined below. Similarly to the example of Section 6.1 let

$$\varepsilon(\boldsymbol{y}) = \frac{\prod_{k=1}^2 \sqrt{2} + \sin(2\pi y_k)}{\sqrt{2}} \qquad \text{and} \qquad \nu(\boldsymbol{y}) = \frac{2}{\prod_{k=1}^2 \sqrt{2} + \sin(2\pi y_k)},$$

such that $\varepsilon^{\mathrm{eff}} = I_2$, $\nu^{\mathrm{eff}} = 1$ and for $\boldsymbol{f}(\boldsymbol{x}) = -\big(\cos(\pi x_1)\sin(\pi x_2), \sin(\pi x_1)\cos(\pi x_2)\big)^T$ we have $\boldsymbol{e}^{\mathrm{eff}}(\boldsymbol{x}) = -\boldsymbol{f}(\boldsymbol{x})$.

For this problem we consider three instances of the FE-HMM scheme. For the first two instances we use first order elements for both the macro and the micro solvers, while for the computations we use different quadrature formulas. The formulas are given in Table 2. While the first quadrature formula (QF_1) is only exact for $\mathcal{P}^1(\hat{K})$, the second one (QF_2) is also exact for $\mathcal{P}^2(\hat{K})$. For both FE-HMM schemes we use the same macro and micro meshes. The refinement strategy is the same as above, i.e. $H \sim h^2$. While the error between $\boldsymbol{e}^{\mathrm{eff}}$ and $\boldsymbol{e}_H^{\mathrm{HMM}}$ does not decay for the FE-HMM with (QF_1), we get the expected first order convergence for (QF_2), see Figure 3. The reason therefore, is that assumption (Q) is not fulfilled for FE-HMM with (QF_1). As mentioned before, we see here that (Q) is an assumption on the quadrature formula.

For the last instance of the FE-HMM scheme we use again the quadrature formula (QF_2). However, for the macro solver we use Nédélec edge element of order two. For the micro solvers we use still first order elements. Now, $\inf_{\boldsymbol{v}_H \in \boldsymbol{V}_{H,0}} \|\boldsymbol{e}^{\mathrm{eff}} - \boldsymbol{v}_H\|_{\mathbf{curl},\Omega} \in \mathcal{O}(H^2)$. Hence, we refine the macro and the micro mesh simultaneously with $H \sim h$. In the numerical results we retrieve second order convergence, see Figure 3. Note that the convergence order is not lowered by the use of the quadrature formula (QF_2). This is remarkable, since only $\mathrm{err}_{\mathrm{mac}}^{\nu} = 0$, whereas $(\varepsilon^{\mathrm{eff}} \boldsymbol{v}_H \,|\, \boldsymbol{w}_H)_{0,\Omega}$ is not computed exactly using (QF_2). We see, that it is not necessary that the macro error vanishes to retrieve

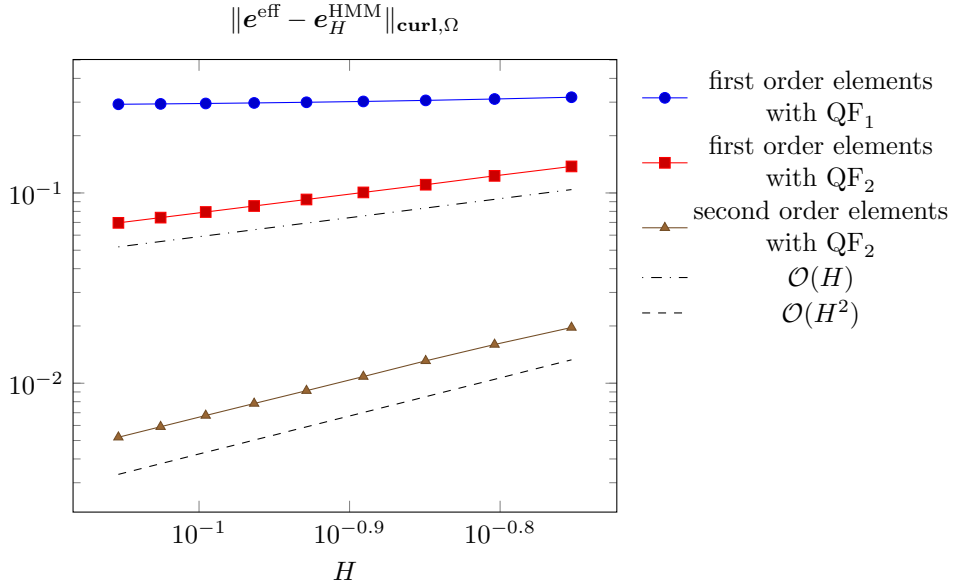

Figure 3: Error between the exact effective solution $\boldsymbol{e}^{\text{eff}}$ and the three FE-HMM approximations for different mesh sizes H of the macro solver. With the quadrature formula (QF_1) no convergence can be observed, since the assumption (Q) does not hold. For (QF_2) the FE-HMM converges with the expected convergence order 1 or respectively 2, in accordance to the order of the chosen macro solver. The micro mesh size is refined simultaneously.

an optimal convergence order. It is enough if they converge to zero sufficiently fast as $H \to 0$, see Theorem 11.

6.3. Stratified locally periodic medium

For the final experiment we consider a stratified medium as in Section 6.2, that is only locally periodic. More precisely, we let $\varepsilon^\eta(\boldsymbol{x}) = I_2$ and

$$\nu^\eta(\boldsymbol{x}) = \frac{4(1+x_1)(1+x_2)}{\big(2+\sin\frac{2\pi x_1}{\eta}\big)\big(2+\sin\frac{2\pi x_2}{\eta}\big)}, \qquad \text{with } \eta = \frac{1}{100}.$$

The material is chosen such that the effective permittivity and permeability tensors can still be computed analytically, due to its simple structure. We get $\varepsilon^{\text{eff}}(\boldsymbol{x}) = I_2$ and $\nu^{\text{eff}}(\boldsymbol{x}) = (1+x_1)(1+x_2)$. As before, $\Omega = (0,1)^2$ and $\omega = 1$. However, the right-hand side is now given by $\boldsymbol{f}$ such that

$$f_1(\boldsymbol{x}) = f_2(\boldsymbol{x}) = \exp\big(-10(x_1-0.5)^2 - 10(x_2-0.5)^2\big).$$

For this experiment we use again first order elements and the quadrature formula (QF_2) (see Table 2) for the HMM scheme. We choose uniform meshes for the macro and the micro solver with 10, respectively 4 elements per side. Thus we have 200 macro and 32 micro elements. Since there is no closed formula for the effective solution, we compare the FE-HMM solution $\boldsymbol{e}_H^{\text{HMM}}$ with an FEM approximation of the effective equation $\boldsymbol{e}_H^{\text{eff}}$

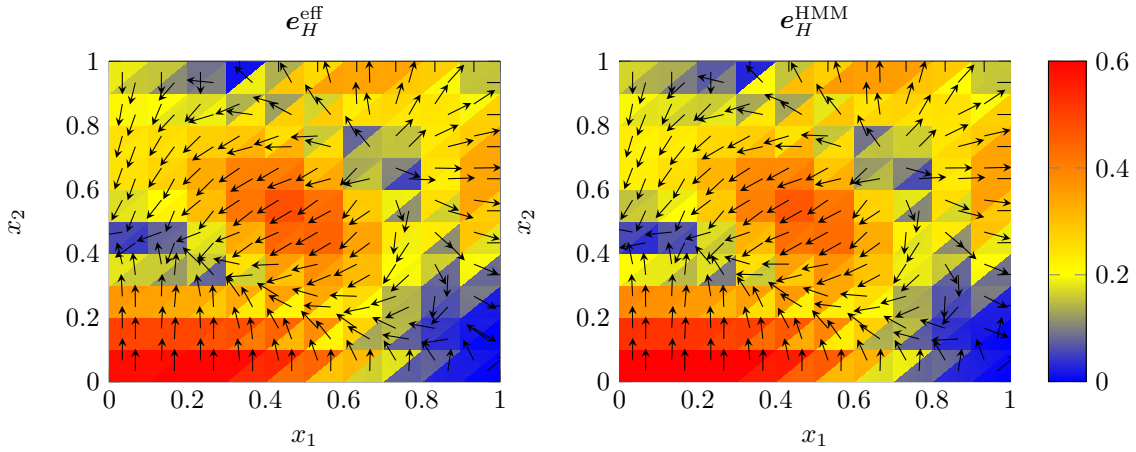

Figure 4: FEM solution $\boldsymbol{e}_H^{\text{eff}}$ of the homogenized Maxwell's equations (left) and FE-HMM solution (right). The modulus of these electric fields is color coded and the modulus indicated by the arrows. Although only 32 elements per micro problem where used, the FE-HMM solution approximates well the effective behavior.

on the macro mesh. To compute $\boldsymbol{e}_H^{\text{eff}}$ we apply an improved quadrature formula (order 10 and 21 quadrature nodes per element). Despite the small number of elements, $\boldsymbol{e}_H^{\text{HMM}}$ aproximates $\boldsymbol{e}_H^{\text{eff}}$ well, as it can be seen on Figure 4. The relative error between $\boldsymbol{e}_H^{\text{eff}}$ and $\boldsymbol{e}_H^{\text{HMM}}$ measured in the $\boldsymbol{H}(\mathbf{curl};\Omega)$-norm is 11.3%.

Acknowledgement

This work was financially supported by the SNFS (Project 151906), the ANR META-MATH (Project ANR-11-MONU-016), the Klaus Tschira Stiftung, and the Deutsche Forschungsgesellschaft (DFG) through CRC 1173.

References

[1] P. Ciarlet, Jr., On the approximation of electromagnetic fields by edge finite elements. part 1: Sharp interpolation results for low-regularity fields, Comput. Math. Appl. 71 (1) (2016) 85–104.
[2] A. Sihvola, Electromagnetic Mixing Formulas and Applications, Vol. 47 of Electromagnetic Waves Series, IEE, 1999.
[3] A. Bensoussan, J.-L. Lions, G. Papanicolaou, Asymptotic Analysis for Periodic Structures, AMS Chelsea Publishing, Providence, RI, 2011, corrected reprint of the 1978 original.
[4] V. V. Jikov, S. M. Kozlov, O. A. Oleinik, Homogenization of Differential Operators and Integral Functionals, Springer-Verlag, 1994.
[5] N. Wellander, Homogenization of the Maxwell equations: Case i. linear theory, Appl. Math. 46 (1) (2001) 29–51.
[6] N. Wellander, Homogenization of the Maxwell equations: Case ii. nonlinear conductivity, Appl. Math. 47 (3) (2002) 255–283.
[7] N. Wellander, G. Kristensson, Homogenization of the Maxwell equations at fixed frequency, SIAM J. Appl. Math. 64 (1) (2003) 170 –195.
[8] L. Cao, Y. Zhang, W. Allegretto, Y. Lin, Multiscale aymptotic method for Maxwell's equations in composite materials, SIAM J. Numer. Anal. 47 (6) (2010) 4257–4289.

[9] C. Engström, D. Sjöberg, On two numerical methods for homogenization of Maxwell's equations, J. of Electromagn. Waves and Appl. 21 (13) (2007) 1845–1856.
[10] D. Sjöberg, C. Engström, G. Kristensson, D. Wall, N. Wellander, A Floquet-Bloch decomposition of Maxwell's equations applied to homogenization, Multiscale Model. Simul. 4 (1) (2005) 149–171.
[11] T. Y. Hou, X.-H. Wu, A multiscale finite element method for elliptic problems in composite materials and porous media, J. Comput. Phys. 134 (1) (1997) 169–189.
[12] Y. Efendiev, T. Y. Hou, Multiscale Finite Element Methods, Springer-Verlag, 2009.
[13] W. E, B. Engquist, The heterogeneous multiscale methods, Commun. Math. Sci. 1 (1) (2003) 87–132.
[14] A. Abdulle, W. E, B. Engquist, E. Vanden-Eijnden, The heterogeneous multiscale method, Acta Numer. 21 (2012) 1–87.
[15] J. Buša Jr., Nonlinear and multiscale problems in low-frequency electromagnetism, Ph.D. thesis, Ghent University, Faculty of Sciences, Numerical Analysis and Mathematical Modelling Research Group (2009).
[16] J. Buša Jr., V. Melicher, Heterogeneous multiscale method in eddy currents modeling, in: Proceedings of ALGORITHMY, 2009.
[17] P. Henning, M. Ohlberger, B. Verfürth, A new heterogeneous multiscale method for time-harmonic Maxwell's equations, SIAM J. Numer. Anal. (accepted for publication).
[18] A.-S. Bonnet-Ben Dhia, J. P. Ciarlet, C. M. Zwölf, Time harmonic wave diffraction problems in materials with sign-shifting coefficients, J. Comput. Appl. Math. 234 (2010) 1912–1919, Corrigendum p. 2616.
[19] P. Ciarlet, Jr., T-coercivity: Application to the discretization of Helmholtz-like problems, Comput. Math. Appl. 64 (1) (2012) 22–34.
[20] X. Yue, W. E, The local microscale problem in the multiscale modeling of strongly heterogeneous media: Effects of boundary conditions and cell size, J. Comput. Phys. 222 (2) (2007) 556–572.
[21] G. Nguetseng, A general convergence result for a functional related to the theory of homogenization, SIAM J. Math. Anal. 20 (3) (1989) 608–623.
[22] G. Allaire, Homogenization and two-scale convergence, SIAM J. Math. Anal. 23 (6) (1992) 1482–1518.
[23] N. Svanstedt, N. Wellander, A note on two-scale limits of differential operators, Tech. Rep. 19, Department of Mathematics, Chalmers University of Technology, Göteborg, Sweden (2001).
[24] D. Cioranescu, P. Donato, An Introduction to Homogenization, Vol. 17, Oxford, University Press, 1999.
[25] S. Guenneau, F. Zolla, A. Nicolet, Homogenization of 3d finite photonic crystals with heterogeneous permittivity and permeability, Waves in Random and Complex Media 17 (4) (2007) 653–697.
[26] A. Abdulle, The finite element heterogeneous multiscale method: A computational strategy for multiscale PDEs, GAKUTO Internat. Ser. Math. Sci. Appl. 31 (2009) 133–181.
[27] P. Monk, Finite Element Methods for Maxwell's Equations, Oxford, University Press, 2003.
[28] Z. Chen, Q. Du, J. Zou, Finite element methods with matching and nonmatching meshes for Maxwell equations with discontinous coefficients, SIAM J. Numer. Anal. 37 (5) (2000) 1542–1570.
[29] A. Abdulle, A. Nonnenmacher, A short and versatile finite element multiscale code for homogenization problems, Comput. Methods Appl. Mech. Engrg. 198 (2009) 2839–2859.
[30] A. Abdulle, The role of numerical integration in numerical homogenization, ESAIM: Proceedings 50 (2015) 1–20.
[31] P. Solin, K. Segeth, I. Dolezel, Higher-order finite element methods, Studies in Advanced Mathematics, CRC Press, 2003.
[32] P. G. Ciarlet, The Finite Element Method for Elliptic Problems, Vol. 40 of Classics in applied mathematics, SIAM, 2002, reprint from 1978s original.
[33] A. Ern, J.-L. Guermond, Theory and Practice of Finite Elements, Vol. 159 of Applied Mathematical Sciences, Springer-Verlag, New York, 2004.
[34] A. Bermúdez, R. Rodríguez, P. Salgado, Numerical treatment of realistic boundary conditions for the eddy current problem in an electrode via Lagrange multipliers, Math. Comp. 74 (249) (2005) 123–151.
[35] A. Bonito, J.-L. Guermond, F. Luddens, Regularity of the Maxwell equations in heterogeneous media and Lipschitz domains, J. Math. Anal. Appl. 408 (2) (2013) 498–512.
[36] F. Hecht, New development in FreeFem++, J. Numer. Math. 20 (3-4) (2012) 251–265.